

Doctorate Dissertation

博士論文

Piwi nuclear localization and its regulatory
mechanism in *Drosophila* ovarian somatic cells

(ショウジョウバエ Piwi-piRNA 複合体の
核局在制御機構の解析)

A Dissertation Submitted for Degree of Doctor of Philosophy

December 2017

平成 29 年 12 月 博士 (理学) 申請

Department of Biological Sciences, Graduate School of Science,

The University of Tokyo

東京大学大学院理学系研究科生物科学専攻

Ryu Yashiro

八代 龍

Contents

Abstract.....	4
Abbreviations.....	9
Introduction.....	12
Small RNAs.....	13
piRNAs.....	15
piRNA biogenesis.....	16
Transcriptional transposon silencing by Piwi.....	18
Possibility of Imp α involved in the Piwi nuclear localization.....	19
<i>Drosophila</i> Imp α	20
The aim of this study.....	22
Summary of this study.....	23
Materials and Methods.....	25
Cell culture.....	26
Plasmid transfection and RNAi.....	26
Production of monoclonal antibodies for Importin α 1, Importin α 2 and Importin α 3.....	28
Immunofluorescence.....	29
Western blotting.....	30
Plasmid rescue assay.....	31
Immunoprecipitation.....	32
Estimation of Imp α protein levels in OSCs.....	33

Limited proteolysis assay.....	34
Epitope analysis.....	34
Detection of small RNAs associated with Piwi.....	35
Plasmid construction.....	36
Results.....	40
Antibody production.....	41
Quantification of Imp α 1, Imp α 2, Imp α 3 protein level in OSC42	
Piwi mislocalized only in Imp α 2 or Imp α 3 depletion and the	
mislocalization was not affected for piRNA loading.....	43
All three Imp α individually rescued the Piwi mislocalization	
that was caused by Imp α 2 or Imp α 3 depletion in OSC.....	44
The nuclear localization of the cargo protein containing	
SV40-NLS was not affected by Imp α depletion.....	45
Determination of Piwi-NLS.....	46
Piwi-NLS is a bipartite NLS.....	47
Cargo protein with Nucleoplasmin NLS (NP-NLS) behaved	
similarly to Piwi in Imp α -depleted OSC.....	48
‘Protein X’ that may hide to prevent Imp α binding prior to	
Piwi-piRNA loading.....	49
Addition of another Piwi-NLS leads Piwi to be localized to the	
nucleus in a piRNA-independent manner.....	50
A conformational change induced by piRNA loading might	

lead Piwi-NLS to be exposed to Imp α	51
Imp α and Piwi binding activity is depend on piRNA binding	53
sDMA modification and phosphorylation of Piwi have little impact on Piwi nuclear localization.....	54
Discussion.....	56
<i>Drosophila</i> Imp α monoclonal antibodies.....	57
Imp α is a nuclear import factor of Piwi.....	58
Piwi may change its conformation whether piRNA is loaded or not.....	58
Cargos often require a specific Imp α , but Piwi does not.....	59
Why does Piwi have a bipartite NLS?.....	60
Conclusion.....	62
References.....	65
Figures.....	77
Tables.....	104
Acknowledgements.....	107

Abstract

ショウジョウバエ Piwi-piRNA 複合体の核局在制御機構の解析

平成 27 年度入学 八代 龍

指導教員 塩見 美喜子

○ 本研究の背景

ショウジョウバエ卵巣内体細胞で発現する Piwi タンパク質は piRNA と piRISC を形成し、トランスポゾン転写レベルを抑制することによって生殖ゲノムの品質を守る。Piwi や piRNA の機能喪失はトランスポゾンの脱抑制、ひいては生殖ゲノム損傷を引き起こし、配偶子形成不全や不妊を導く。これまでのショウジョウバエ卵巣および卵巣由来体細胞株 OSC を用いた解析から、N 末端 72 アミノ酸を欠失した Piwi 変異体は piRNA に結合するが核に局在しないこと、また piRNA に結合しない Piwi 変異体は核局在化シグナル (NLS) が存在するにも関わらず核に局在しないことが示された。つまり、Piwi の核局在には、Piwi の N 末端 72 アミノ酸と piRNA 結合の両者が必要であるといえる。しかし、Piwi の核局在に関わる核移行システムの実態、および piRNA の依存性の仕組みは未だ不明である。そこで、本研究において、私はこれらの疑問に対する解答を得るため、OSC を用いて生化学的な解析を進めることにした。

○ 結果・考察

Piwi の N 末端 72 アミノ酸は塩基性アミノ酸に富む。塩基性アミノ酸に富む NLS を持つタンパク質の核移行を担う因子として Importin α (Imp α) が知られる。そこで Imp α に着目して実験を進めることにした。ショウジョウバエ Imp α 遺伝子は Imp $\alpha 1$ 、Imp $\alpha 2$ 、Imp $\alpha 3$ の 3 つある。各 Imp α タンパク質に対するモノクローナル抗体を作製し、OSC 内の発現量を観察したところ、Imp $\alpha 1$ の発現が非常に少ないのに対し、Imp $\alpha 2$ の発現は高く、Imp $\alpha 3$ は中程度であった。各 Imp α 遺伝子の発現を RNAi によってノックダウン (KD) した OSC 細胞で Piwi を強制発現させ、その細胞内局在

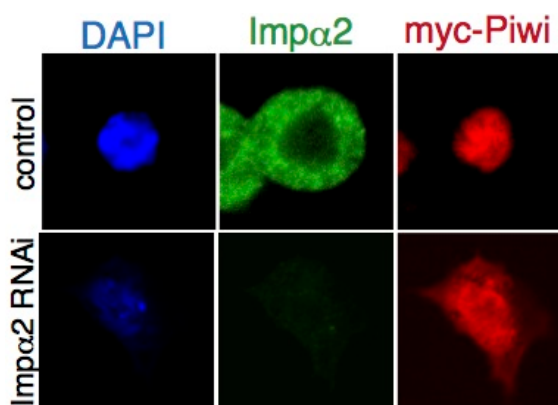


図 1. Piwi の細胞内局在における Imp α の依存性

Imp $\alpha 2$ を KD することで Piwi の核局在が阻害された。青色は DAPI、緑色は Imp $\alpha 2$ 、赤色は myc-Piwi を示す。

を観察したところ、Imp α 1 の KD は Piwi の発現に影響を及ぼさなかったが、Imp α 2 と Imp α 3 の KD は Piwi の核輸送を阻害した (図 1)。一方、SV40-NLS をもつタンパク質はいずれの場合においても影響を受けなかった。この結果は Piwi の核移行には SV40-NLS をもつタンパク質と異なり、Imp α 2 と Imp α 3 の両者を必要とする可能性を示唆した。しかし Imp α 2 もしくは Imp α 3 を KD した細胞において、各 Imp α メンバーの強制発現によって Piwi の核移行が復活したため、この可能性は排除できた。またこの結果は、Piwi の核移行はいずれの Imp α メンバーによっても担われる可能性を示唆した。続いて、Piwi の NLS 配列の決定を試みた。Piwi の N 末端 36 アミノ酸を欠失した Piwi 変異体は核移行せず、この配列を付加した EGFP は核のみに局在した。この領域の塩基性アミノ酸の点変異解析を進めたところ、Piwi-NLS は SV40-NLS とは異なり双極型であることが判明した。

Piwi の核移行は Piwi-NLS だけでなく piRNA の結合を必要とする。そこで、Piwi が piRNA に結合しない場合、Piwi-NLS は何者かによって隠されているため Imp α が結合できず Piwi は細胞質に留まるが、一旦 piRNA が結合すると Piwi に構造変化が生じ Piwi-NLS が露出するため、Imp α が Piwi を核に移行させることが出来るようになるという仮説を立てた。これを検証するため、まずプロテアーゼ限定分解実験を行った。piRNA に結合していない Piwi-N 末端はキモトリプシンに対して耐性を示した一方、piRNA に結合した Piwi の N 末端は感受性を示した。この結果は piRNA の有無によって Piwi の構造が変わり、Piwi の N 末端つまり Piwi-NLS の露出度合いが変化することを示唆している。Piwi-NLS を Piwi が piRNA に結合するまで隠すものは一体何なのか。1 つ目の仮説として、未知因子 X が Piwi-NLS に結合するという可能性を考えた。しかし、Piwi-NLS を SV40-NLS に置換した Piwi 変異体も piRNA 生合成の阻害によって核移行に影響が出たことを考えるとその可能性は考えにくい。そこで 2 つ目の仮説として、Piwi-NLS は Piwi 自身によって隠されているという可能性を考えた。これを実証するため、Piwi の N 末端に Piwi-NLS をもう 1 つ付加した Piwi 変異体を作成し、その核局在の piRNA 依存性を確認した。その結果、この Piwi 変異体は piRNA 非依存的に核局在を示した。これらの結果より、piRNA が結合していない場合、Piwi 自身が Piwi-NLS を隠すことによって Piwi の核局在を負に制御する可能性が強く示唆された。

○ 総括

ショウジョウバエ卵巣由来体細胞株 OSC を用いた生化学的な解析により、以下を明らかにした。① Piwi の核局在は Imp α によって担われていること、② Piwi-NLS は Piwi の N 末端の 36 アミノ酸であること、③ Piwi-NLS は双極型であることが判明した。また、④ Piwi が piRNA と結合しない時は、Piwi 自身が Piwi-NLS を隠すことによって Imp α との結合を阻害していること、しかし、⑤ 一旦 Piwi に piRNA が結合すると、Piwi に構造変化が生じ、Piwi-NLS が露出するため Imp α が結合できる様になり、核移行するという可能性が示唆された。Piwi-NLS が SV40-NLS と異なり Imp $\alpha 3$ の KD に強い感受性を示す理由は不明であるが、双極型ヌクレオプラスミン NLS をもつタンパク質も Piwi のように Imp $\alpha 3$ の KD に強い感受性を示したため、Imp α は単極型 NLS を優先して核に輸送する可能性が考えられた。

Abstract

In *Drosophila* ovarian somatic cells (OSCs), Piwi represses transposons transcriptionally to maintain genome integrity. Piwi nuclear localization requires the N-terminal region and piRNA loading of Piwi. However, the nuclear import machinery and the mechanism underlying the piRNA loading-dependency remain unknown. Here we showed that Importin α (Imp α) plays a pivotal role in Piwi nuclear localization and that Piwi has a classical bipartite nuclear localization signal (NLS) at the N-terminal end. Imp α 2 and Imp α 3 were fairly highly expressed in OSCs, whereas the last member Imp α 1 was the least expressed. Loss of Imp α 2 or Imp α 3 in OSCs caused mislocalization of Piwi, but not of SV40-NLS-cargo, to the cytoplasm. The overexpression of Imp α 1, Imp α 2, or Imp α 3 rectified Piwi nuclear localization in the OSCs. Extension of Piwi-NLS by fusing an additional Piwi-NLS led Piwi to be imported to the nucleus in a piRNA-independent manner, whereas replacement of Piwi-NLS with SV40-NLS failed to do so. Limited proteolysis analysis suggested that the N-terminal approximately 200 residues of Piwi were hidden when not loaded with piRNAs, but piRNA loading triggered conformational change in Piwi, exposing the N-terminus to the environment. These results suggest that Piwi autoregulates its nuclear localization by exposing the NLS to Imp α exclusively upon piRNA loading.

Abbreviations

Abbreviations

Abbreviation	Full name
Ago	Argonaute
APS	Ammonium Peroxodisulfate
ARM	Armadillo
Armi	Armitage
Aub	Aubergine
BSA	Bovine Serum Albumin
CBB	Coomassie Brilliant Blue
DNA	Deoxyribonucleic acid
DTT	Dithiothreitol
EGFP	Enhanced Green Fluorescent Protein
FBS	Fetal Bovine Serum
FE	Fly Extract
GST	Glutathione S-transferase
HRP	Horseradish peroxidase
IF	Immunofluorescence
IgG	Immunoglobulin G
IgM	Immunoglobulin M
Imp	Importin
IP	Immunoprecipitation
kb	Kilobase
KD	Knock down
kDa	Kilodalton
KOAc	Potassium acetate
Luc	Luciferase
MgOAc	Magnesium acetate
miRNA	Micro RNA
mRNA	Messenger RNA
ncRNA	Non-coding RNA
n.i.	Non immune

NLS	Nuclear Localization Signal
NP	Nucleoplasmin
NP40	Nonidet P-40
nt	Nucleotide
OSC	Ovarian Somatic Cell
PAGE	Polyacrylamide gel electrophoresis
piRNA	PIWI-interacting RNA
Piwi	P-element induced wimpy testis
pre-miRNA	Precursor miRNA
pri-miRNA	Primary miRNA
RISC	RNA-induced silencing complex
RNA	Ribonucleic acid
RNAi	RNA interference
S2	Schneider 2
SDS	Sodium lauryl sulfate
SDS-PAGE	(refer to each abbreviation)
siRNA	Small-interference RNA
SV40-NLS	SV40 large T-antigen NLS
TE	Transposable element
TEMED	Tetramethylethylenediamine
T-PBS	Phosphate buffered saline with Tween20
Tris	Tris (hydroxymethyl) aminomethane
Yb	Female sterile (1) Yb
Zuc	Zucchini

Introduction

Introduction

Small RNAs

Living cells of eukaryotes express a large variety of RNAs including protein-coding mRNAs, ribosomal RNAs, transfer RNAs, small nuclear RNAs (snRNAs), small nucleolar RNAs (snoRNAs), and even RNAs smaller than snRNAs and snoRNAs, which are collectively termed “small RNAs”. The sizes of these small RNAs are normally 20-35 nucleotides (nts) long, and the size range may vary among organisms. For example, *Drosophila melanogaster*, the experimental model system that I have been using in the laboratory, small RNAs are normally 20-30 nts long. The function of small RNAs is to repress gene expression. Without the function of small RNAs, living organisms cannot develop properly, which is often life threatening. Therefore, small RNAs are indispensable for maintaining the life of organisms. Small RNAs in animals can be divided into three groups, microRNAs (miRNA), small interference RNAs (siRNAs) and PIWI-interacting RNAs (piRNAs) (Eulalio et al. 2008; Iwasaki et al. 2009) (Figure 1). To perform gene silencing, all these small RNAs individually form RNA-induced silencing complexes (RISCs) with members of Argonaute family of proteins in a stoichiometric manner

(Siomi et al. 2011). Then, small RNAs guide the protein partners, i.e., Argonaute proteins, to RNA transcripts arising from target genes through RNA-RNA base-pairings to accomplish the target gene repression (Figure 1).

RISCs containing miRNAs are called miRISCs, which repress protein-coding genes in a spatial-temporal manner, by blocking translation of target mRNAs or facilitating mRNA decay (Vagin et al. 2006; Saito et al. 2006). Exogenous siRNAs such as those arising from viral RNAs upon infection to living cells or double-stranded RNAs artificially introduced into cells can also target protein-coding genes and/or non-coding RNAs, and silence the target genes by cleaving the target gene transcripts. Living cells often express siRNAs endogenously, which are known as endo-siRNAs (Ghildiyal et al. 2009; Kawamura et al. 2008; Watanabe et al. 2008). In *Drosophila*, endo-siRNAs are expressed ubiquitously and mainly repress transposons in somatic cells (Kawamura et al. 2008). However, their abundance is low and so loss of endo-siRNAs only slightly upregulates transposons. piRNAs assemble piRISCs with PIWI proteins (i.e., germline-specific Argonaute proteins). *Drosophila* expresses three members of PIWI proteins, Piwi, Aubergine (Ago3) and Ago3 (Cox et al. 1998; Schmidt et al. 1999; Li et al. 2009; Nagao et al. 2011).

piRNAs

While miRNAs and siRNAs are expressed ubiquitously, piRNAs are expressed specifically in the germline. The sequences of piRNAs are mostly complementary to transposon mRNAs, particularly in *Drosophila*, so piRNAs act as antisense oligos to repress transposons. A small fraction of piRNAs is complementary to protein-coding mRNAs. For example, piRNAs arising from the repetitive *suppressor of stellate* [*su(ste)*] locus in the *Drosophila* genome, on chromosome X, are complementary to *Stellate* mRNA encoding a protein homologous to β -subunit of Casein Kinase II (Livak 1990). Although *Stellate* mRNAs are expressed in fly testis, accumulation of *Stellate* protein in testis severely interferes with spermatogenesis. To avoid such unwanted situation, *su(ste)*-piRNAs assemble piRISCs with Aub and repress the *Stellate* gene by cleaving *Stellate* mRNAs in the cytoplasm.

piRNAs targeting transposons are primarily produced from intergenic DNA elements termed piRNA clusters, which are filled with transposon remnants. Those transposon fragments are embedded into piRNA clusters in a direction against the direction of transcription. Therefore, piRNAs arising from the piRNA clusters become naturally antisense, after maturation, to parental transposon mRNAs. piRNA clusters are transcribed by RNA polymerase II. Therefore, the resultant transcripts,

i.e., piRNA precursors are single-stranded. Therefore, piRNA processing occurs independent of Dicer, the RNase III domain-containing nuclease necessary for siRNA and miRNA biogenesis (Bernstein et al. 2001). The precursors of siRNAs and miRNAs are long double-stranded (ds) RNAs and pre-miRNAs (i.e., precursors of miRNAs), the latter of which form unique hairpin structures, respectively. Dicer processes long dsRNAs from both ends to ~21 nt-long siRNAs. miRNAs are produced from the stem regions of hairpin structures within pre-miRNAs. pre-miRNAs arise from pri-miRNAs (i.e., primary miRNA precursors), the nascent transcripts of miRNA genes, in a manner depending on Drosha, another RNase III domain-containing nuclease. Conversion of pre-miRNA to mature miRNA requires Dicer.

Loss-of-function mutations of PIWI proteins and piRNA factors cause defects in the genome surveillance system, leading to transposon derepression, failures in gametogenesis, and infertility (Grimson et al. 2008; Khurana and Theurkauf 2010) (Figure 2).

piRNA biogenesis

Transposon-targeting piRNAs are primarily produced from piRNA clusters. The piRNA clusters in *Drosophila* are divided into un-strand and

dual-strand piRNA clusters. Uni-strand clusters, which are transcribed in one fixed direction, are used mainly in the ovarian somatic cells, while dual-strand clusters, which are transcribed in both directions, are used mainly in the germ cells (Malone et al. 2009; Yamashiro and Siomi 2018). In both cases, nascent transcripts of the clusters serve as piRNA precursors. How each cluster is selected as the piRNA genomic source in the cells remains largely unknown.

In ovarian somatic cells, RNA transcripts of uni-strand piRNA clusters are selectively bound with fs(1)Yb protein (Yb) and processed into piRNAs at Yb body, perinuclear foci known as piRNA processing center (Figure 4). Yb recognizes and binds the *cis*-regulatory elements embedded in the cluster transcripts. Multiple piRNA factors including Armitage, Vreteno and Zucchini (Zuc) are involved in the piRNA processing (Nishimasu et al. 2012). The mature piRNAs are loaded onto Piwi protein and the resultant piRISC is translocated to the nucleus to repress transposons at the transcriptional levels. piRNAs are not loaded onto Aub and Ago3 in ovarian somatic cells because they are not expressed in the cells (Figure 3).

In germ cells, RNA transcripts of the dual-strand piRNA clusters give rise to primary piRNAs. How the RNA transcripts are selected to be piRNA precursors and how the processing occurs largely remain unknown. The primary piRNAs are loaded onto Piwi and Aub. Piwi-piRISC is

transported to the nucleus, as in ovarian somatic cells, and silence transposons at the transcriptional levels. Aub-piRISC remains to be in the cytoplasm and represses transposons by cleaving the mRNAs using its own endonuclease activity known as Slicer. Cleaved RNAs now serve as precursors of secondary piRNAs, which are loaded onto Ago3. Aub- and Ago3-bound piRNAs are mainly antisense and sense to transposon-coding sequences, respectively, and Aub and Ago3 reciprocally cleave transposon mRNAs and antisense transcripts, respectively. As indicated above, the resultant RNA fragments are further processed to mature piRNAs; thereby, Aub/Ago3-Slicer-dependent transposon silencing in germ cells is considered to be coupled with piRNA biogenesis (Brennecke et al. 2007; Gunawardane et al. 2007; Nishida et al. 2007; Li et al. 2009).

Transcriptional transposon silencing by Piwi

Piwi in both germ cells and ovarian somatic cells is localized to the nucleus and silences transposons transcriptionally by inducing heterochromatinization at the target loci with co-factors such as Panoramix/Silencio, Asterix/GTSF1, Maelstrom and linker histone H1 (Kalmykova et al. 2005; Saito et al. 2006; Saito et al. 2010; Sienski et al. 2012; Czech et al. 2013; Dönertas et al. 2013; Handler et al. 2013; Le

Thomas et al. 2013; Muerdter et al., 2013; Ohtani et al. 2013; Sienski et al. 2015; Yu et al. 2015; Iwasaki et al. 2016) (Figure 5). Piwi nuclear localization requires both the N-terminal region of Piwi and piRNA loading onto Piwi (Saito et al. 2009; Olivieri et al. 2010; Klenov et al. 2011). This layered, “gatekeeping” mechanism ensures Piwi-piRISC-mediated nuclear transposon silencing, because piRNA-free Piwi in the nucleus would be useless without no ability to find its targets, while piRNAs left alone in the cytoplasm are destined to be degraded due to lack of Piwi, the binding partner (Ishizu et al. 2011). However, how piRNA loading-dependent Piwi nuclear localization is regulated mechanistically is still unclear. The nuclear import machinery required for Piwi nuclear import also remains to be undetermined.

Possibility of Imp α involved in the Piwi nuclear localization

The N-terminal region of Piwi, which has been shown to be necessary for its nuclear import, is rich in basic residues, a characteristic typical of classical nuclear localization signals (NLSs) whose nuclear import is mediated by an Importin α/β (Imp α/β) heterodimer (Görlich et al. 1998; Stewart et al. 2007) (Figure 6). The NLS of SV40 large T antigen (SV40-NLS) (PKKKRKV) (Kalderon et al. 1984) and that of *Xenopus*

Xenopus laevis nucleoplasmin (NP-NLS) (KRPAATKKAGQAKKKK) (Robbins et al. 1991) are the prototypic monopartite and bipartite NLSs, respectively (Goldfarb et al. 2004; Stewart et al. 2007) (Figure 6). Monopartite NLSs consist of a single stretch of basic residues, while bipartite NLSs contain two stretches of basic residues with a linker region between them. In the Imp α / β pathway, the adaptor molecule Imp α protein first binds cargos in the cytoplasm through their NLSs. Then, Imp β associates with the heterodimer through the Imp β binding (IBB) domain of Imp α to assemble a NLS-cargo/Imp α /Imp β trimeric complex, which facilitates the nucleocytoplasmic translocation of the complex across the nuclear pores located on the nuclear envelope (Figure 6). Upon transport, RanGTP in the nucleus binds and disassembles the complex, releasing the cargos to the nucleoplasm where they exert their nuclear functions (Görlich 1998; Stewart et al. 2007). Interestingly, these transport system mediated by Imp α and Imp β is highly conserved for not only human, mouse or rat but also worm, fly or yeast.

***Drosophila* Imp α**

Imp α firstly purified from *Xenopus laevis* and 44% of its sequence was the same as Srp1 of yeast, which is known as Imp α of yeast and

localized near nuclear pore complex (Görlich et al. 1994). Generally speaking, members of the Imp α family of proteins can be divided into three phylogenetic clades $\alpha 1$, $\alpha 2$, and $\alpha 3$ (Mason et al. 2009; Pumroy and Cingolani 2015) (Figure 7). *Drosophila* contains a single representative of each clade, Imp $\alpha 1$, Imp $\alpha 2$, and Imp $\alpha 3$ (Kussel and Frasch 1995; Török et al. 1995; Mason et al. 2002; Mason et al. 2003; Goldfarb et al. 2004) (Figure 7). All Imp α proteins contain one IBB domain at the N-terminal end, and the rest of the sequence contains ten Armadillo (ARM) repeats, which were originally identified in the protein encoded by the *Drosophila* segment polarity gene *armadillo* (Riggelman et al. 1989). While the IBB domain binds Imp β during nuclear import through the nuclear pore, the ARM repeats assemble a scaffold structure that can accommodate monopartite or bipartite NLS (Conti et al. 1998; Fontes et al. 2003). When the ARM repeats are not bound with cargos, the IBB domain binds the ARM repeats intramolecularly, autoinhibiting nuclear import of cargo-free Imp α (Kobe 1999; Stewart 2007). *Drosophila* possibly contains a fourth Imp α member, Imp $\alpha 4$, which, however, lacks the IBB domain and is testis specific (Phadnis et al. 2011). A single Imp β gene known as *ketel* was found in the *Drosophila* genome (Lippai et al. 2000). *Drosophila Imp $\alpha 1$* null flies developed to adulthood, but showed severe defects in gametogenesis and infertility (Ratan et al. 2008). Similarly, homozygous *Imp $\alpha 2$* mutants developed normally to adulthood, but mutant females, and

not males, were completely sterile (Mason et al. 2002). Imp α 3 mutants showed embryonic lethality (Mason et al. 2003). Here I mainly described *Drosophila* Imp α , however these systems and characters are highly conserved on many species.

The aim of this study

On the basis of all these earlier findings, I speculated that Imp α might be responsible for Piwi nuclear localization. To test this speculation, I first examined the levels of Imp α proteins in cultured OSCs. To this end, I produced monoclonal antibodies for each Imp α member and performed western blotting, which revealed that Imp α 2 and Imp α 3 were fairly highly expressed in OSCs, whereas Imp α 1 was the least expressed. Loss of Imp α 2 or Imp α 3 by RNAi treatment disturbed nuclear localization of Piwi. However, nuclear localization of SV40-NLS-cargo was not affected, suggesting that Piwi-NLS may have lower nuclear localization efficiency than SV40-NLS. I defined the N-terminal 36 residues of Piwi as a bipartite NLS. Interestingly, bipartite NP-NLS-cargo behaved similarly to Piwi in OSCs lacking Imp α 2 or Imp α 3. Imp α proteins may prioritize monopartite NLSs over bipartite NLSs, at least in OSCs. Replacement of Piwi-NLS with SV40-NLS failed to obviate the requirement of piRNA loading in

Piwi nuclear localization. However, Piwi was imported to the nucleus piRNA-independently upon duplication of the Piwi-NLS. Limited proteolysis assays showed that about 200 residues in the N-terminal end of Piwi were inaccessible when Piwi was free from piRNAs, but piRNA loading made the region accessible to the environment, most likely through a conformational change in Piwi. Thus, Piwi autoregulates its nuclear localization by exposing the NLS to Imp α upon piRNA loading. Addition of Piwi-NLS caused the otherwise cytoplasmic Aub to be imported to the nucleus in a piRNA-dependent manner, as was Piwi. The piRNA loading-driven exposure of the N-terminal region may be a common feature in PIWI proteins.

Summary of this study

By performing biochemical analyses using cultured *Drosophila* ovarian somatic cells OSCs, what were unveiled are as follows:

- 1) Nuclear localization of Piwi is mediated by Imp α
- 2) Piwi-NLS is 36 amino acids of Piwi N-terminus.
- 3) Piwi-NLS is a bipartite NLS.
- 4) When Piwi does not form piRISC, Piwi itself hides its NLS intramolecularly and prevents binding to Imp α .

5) Once piRNA is loaded onto Piwi, structural change might occur. Then, its NLS exposes and can be recognized by Imp α .

The character of Piwi-NLS is different from that of SV40-NLS and the reason why Piwi-NLS shows strong sensitivity to Imp α 3 KD is unclear. However, the protein fused with the representative example of a bipartite NLS, Nucleoplasmin NLS, also showed the strong sensitivity to Imp α 3 KD. These results suggest that Imp α imports the cargo protein having a monopartite NLS preferentially to the nucleus.

Materials and Methods

Materials and Methods

Cell culture

OSCs were generated in my laboratory (Saito et al. 2009). The OSC medium has a special ingredient, called fly extract (FE) (Saito et al. 2009). The composition is here: 50mL of FE, 50mL of FBS (ATLAS BIOLOGICALS), 5mL of Glutathione (Sigma Aldrich), 5mL of Insulin (Wako) and 500mL of Shields and Sang M3 insect medium (Sigma Aldrich). OSCs were cultured by this medium on 26°C and passaged twice a week. S2 cells were cultured by Schneider's insect medium (Sigma Aldrich) that is added 50mL of FBS and 5mL of Penicillin-Streptomycin (Gibco) into 500mL of the medium on 26°C. S2 cells were also passaged twice a week.

Plasmid transfection and RNAi

OSCs were transfected by three ways, siRNA transfection, plasmids transfection or siRNA and plasmids simultaneous transfection. Firstly, siRNA transfection method is shown here. siRNAs were designed by

siDirect (<http://sidirect2.rnai.jp/>) and purchased from Sigma Aldrich. siRNAs used in this study are shown in Table1. To perform RNAi, 3×10^6 OSCs and 200 pmol of siRNAs were mixed with 20 μ L of SF Cell Line Solution (Lonza). These cells were transfected by electroporation by Nucleofector 96-well Shuttle system (Lonza). Secondly, plasmids transfection method is shown here. Plasmids used in this study are shown in Table2. Primers used to make these plasmids are also shown in Table2. Procedure of making plasmids was shown at the section ‘Plasmid Construction’. OSCs were re-spread to be a half-confluent of the dish area on next day. 4 / 8 / 16 μ g of plasmids per 2.5cm / 6cm / 10cm dish were mixed with 96 / 192 / 284 μ L of Xfect Transfection Reagent (Clontech). 1.2 / 2.4 / 3.6 μ L of Xfect Polymer (Clontech) was diluted with 98.8 / 197.6 / 296.4 μ L of the same buffer. Then the two solutions were mixed and incubate for 10 minutes. After that, the mixture was dropped onto the cells. Lastly, simultaneous siRNA and plasmid transfection method is shown. 3×10^6 OSCs, 200 pmol of siRNAs and 4 / 8 / 16 μ g of plasmids were mixed with 100 μ L of Cell Line NucleofectorTM Solution V (Lonza). These cells were transfected by electroporation by Nucleofector 2b (Lonza).

Production of monoclonal antibodies for Importin α 1, Importin α 2 and Importin α 3

The first step of antibody production is to inject recombinant proteins into the abdominal cavity of mice. Concretely, each recombinant protein, which is Glutathione S-transferase (GST)-Imp α 1, GST-Imp α 2 and GST-Imp α 3 was purified from *E.coli*. The plasmids used for this experiment were shown in the section 'Plasmid Construction'. These GST recombinant proteins were injected into mice once in two weeks, three times for immunization. After that, a little amount of blood was collected from caudal vein. Then, serum was obtained from blood and checked the reactivity by western blotting using OSC lysates. Once the reactivity was confirmed, these recombinant proteins were injected to knee lymph node to increase the reactivity; this procedure is called 'boost'. A week later from 'boost', the spleen was removed and the cells were fused with mouse myeloma to make hybridoma; this procedure is called 'fusion'. A week later, I performed ELISA for checking the reactivity of hybridomas using supernatant, this is called '1st screening'. The 2nd screening was performed by western blotting. The antibody was also checked by immunofluorescence (IF) and immunoprecipitation (IP) using OSCs. Finally, 'monoclonalization' was performed. The positive hybridomas were diluted and grown up in 96-well plates. The wells that are grown up

from one hybridoma cell were selected and cultured in large scale. Then, cultured media containing monoclonal antibodies were obtained.

Immunofluorescence

OSCs were spread onto MICRO COVER GLASS (MATSUNAMI) and fixed by formaldehyde (Wako) diluted to 4% by PBS for 15 minutes. Then, cells were permeabilized by 0.1% TritonTM X-100 (Sigma Aldrich) for 15 minutes. The primary antibody was applied to cells for 30 minutes. Primary antibodies used in this study were cultured supernatants of anti-Imp α 1 hybridoma cells, anti-Imp α 2 hybridoma cells, anti-Imp α 3 hybridoma cells, a rabbit polyclonal antibody of myc-tag (1:500 dilution) (Sigma Aldrich), anti-Yb mouse monoclonal antibody (1:500 dilution) (Murota et al. 2014). After that, cells were washed for 10 minutes three times. The secondary antibody was applied for 30 minutes. Secondary antibodies used in this study were Alexa 488-conjugated anti-mouse IgM (Abcam), Alexa 488-conjugated anti-mouse IgG (Molecular Probes), Alexa 546-conjugated anti-rabbit IgG (Molecular Probes). Then, cells were washed for 10 minutes three times. Finally cells were mounted by Vectashield with DAPI (Vector laboratories) on MICRO SLIDE GLASS (MATSUNAMI) and observed by LSM710 (ZEISS).

Western blotting

Collected cells were centrifuged at $5000 \times g$, 4°C , for 5 minutes. Supernatant was discarded and cells were mixed with $2 \times$ Sample buffer ($4 \times$ Sample buffer [37.5% glycerol, 8mL of 0.5% Tris-HCl pH6.8 (Upper Tris), 1.6g of SDS and 8mg of Bromophenol blue in 20mL scale], 1M DTT, Distilled water). After 95°C treatment to the cells for 5 minutes, SDS-PAGE was performed. The composition of the gel of SDS-PAGE is shown here. The running gel is composed of 30w/v % Acrylamide / Bis Mixed Solution (Wako), N, N, N', N'-Tetramethylenediamine (TEMED) (Wako), 10% Ammonium peroxydisulfate (APS) (Wako) and 1.5M Tris-HCl pH 8.8 (called Lower Tris). The stacking gel is composed of 30w/v % Acrylamide / Bis Mixed Solution (Wako), N, N, N', N'-Tetramethylenediamine (TEMED) (Wako), 10% Ammonium peroxydisulfate (APS) (Wako) and 0.5M Tris-HCl pH 6.8 (called Upper Tris). The electrophoresis was performed at 200V for 70 minutes and then the gel was transferred to the nitrocellulose membrane (Wako) at an approximate current for 70 minutes. After transfer, the membrane was soaked to 5% skim milk (Morinaga Milk Industry) in T-PBS [0.1% tween 20, 1L of PBS, 9L of distilled water in 10L scale] for 30 minutes. After removing the milk, primary antibodies were applied. The primary antibodies used for western blotting were the cultured supernatants of

anti- $\text{Imp}\alpha 1$ hybridoma cells, anti- $\text{Imp}\alpha 2$ hybridoma cells, anti- $\text{Imp}\alpha 3$ hybridoma cells, a mouse monoclonal antibody of myc-tag (1:1,000 dilution) (obtained from the Developmental Studies Hybridoma Bank), a mouse monoclonal antibody of Flag-tag (1:10,000 dilution) (MBL) and a mouse monoclonal antibody of anti- β -Tubulin (1:1,000 dilution) (obtained from the Developmental Studies Hybridoma Bank). The treatment of primary antibody was for 60 minutes. Then, the antibody was washed for 5 minutes three times. Next, the secondary antibodies were applied. The secondary antibodies used for western blotting were anti-mouse IgG HRP (Cappel) and Mouse TrueBlot ULTRA Anti-Mouse Ig HRP (DOCKLAND). The treatment of secondary antibody was for 30 minutes. Membranes were then washed for 5 minutes four times. The membranes were treated with ClarityTM Western ECL Substrate (BIORAD) and the signals were detected with Molecular Imager ChemiDocTM XRS+ Imaging System (BIORAD).

Plasmid rescue assay

To knockdown *Impa1*, *Impa2* or *Impa3* in OSCs, $\text{Imp}\alpha 1$ -siRNAs, $\text{Imp}\alpha 2$ -siRNAs, and $\text{Imp}\alpha 3$ -siRNAs were introduced separately into OSCs. 2 days later, $\text{Imp}\alpha 1$, $\text{Imp}\alpha 2$ or $\text{Imp}\alpha 3$ were knocked down again to raise the

RNAi effect. Then, plasmid to overexpress flag-Piwi, together with each RNAi-resistant myc-Imp α 1, myc-Imp α 2 or myc-Imp α 3, was co-introduced in OSCs. 1 day later, cells were fixed by 4% formaldehyde and performed Immunofluorescence experiments whose method was described above.

Immunoprecipitation

OSCs were collected and washed twice by PBS. Then, PBS was removed and 1mL of IP buffer (30mM Hepes-KOH (pH 7.3), 5mM DTT, 2mM Mg(OAc)₂, 0.1% NP-40, 150mM KOAc and protease inhibitor) was added. The cells were mixed by 25G FLOW MAX (NIPRO) ten times and 30G Disposable needle (Dentronics) five times with syringe (TERUMO). After that, broken cells were centrifuged for 15 minutes at 13,500rpm, 4°C. The supernatant was collected as lysate. Next, DynabeadsTM protein G (Invitrogen) that was the resins for Immunoprecipitation was washed by IP buffer twice. To bind beads and antibodies, after adding the antibodies, microtubes were rotated for 30 minutes at room temperature. The antibodies used here were the cultured supernatants of anti-Imp α 1 hybridoma cells, anti-Imp α 2 hybridoma cells, anti-Imp α 3 hybridoma cells, anti-Imp β hybridoma cells and mouse IgG as a negative control. After 30 minutes later, buffer was removed and lysates were added there. The tubes

were rotated for 3 hours. 3 hours later, beads were washed 5 times by IP buffer and immunoprecipitated proteins that were caught by beads were extracted by 45 μ L of 2 \times SB for 10 minutes at 70 $^{\circ}$ C. IP was completed. To analyze, 10 μ L of sample was applied to SDS-PAGE and western blotting was performed as described above.

Estimation of Imp α protein levels in OSCs

Recombinant GST-Imp α proteins isolated from *E. coli* and BSA (NEB) were run on protein gels. Protein concentrations of full-length GST-Imp α in each solution were estimated by staining them with CBB to draw the standard curve by using ImageJ (NIH) and comparing them with BSA stained with CBB. Western blotting was then performed using anti-Imp α monoclonal antibodies (produced in this study, shown above) on GST-Imp α and OSC whole lysates. Signal intensity was calculated using ImageJ and amount was estimated from drawn standard curve.

Limited proteolysis assay

To obtain piRNA-free Piwi, Piwi with no tags was expressed in S2 cells by transfection and then immunoprecipitated using anti-Piwi antibody 3G11. Piwi-piRISC was immunoprecipitated from OSCs using 3G11. After extensive washing, chymotrypsin was added to both immunoprecipitated samples to give a final concentration of 2.0 ng/mL. After incubation at 37°C for 30 min, the bead fractions were separated from the supernatants, and both fractions were subjected to western blotting using the other anti-Piwi antibody 4D2. Western blotting was performed as described above.

Epitope analysis

To determine which regions in the Piwi sequence is the epitopes of anti-Piwi monoclonal antibodies 4D2 (Saito et al. 2009), myc-Piwi- Δ N1-20, myc-Piwi- Δ N1-47, myc-Piwi- Δ N20-73, and myc-Piwi- Δ N47-73 were first individually expressed in OSCs by transfection. Myc-Piwi peptides were then immunoprecipitated from each cell lysate using anti-myc antibody and subjected to western blotting using anti-myc-antibody, 3G11 and 4D2. Immunoprecipitation was performed as described above. 3G11 and 4D2

were raised against Piwi N-terminus, Met1-Ile200 (Saito et al. 2009). Then, to determine more detail of the 4D2 antibody epitope, GST-Piwi-NLS-72-120, GST-Piwi-NLS-90-160 and GST-Piwi-NLS-130-200 were purified from *E.coli*. Western blotting was performed by using anti-GST (Cell Signaling) and anti-Piwi 4D2 as described above. GST-Piwi-NLS-200 and GST-Imp α 1 were applied as a positive control and a negative control respectively.

Detection of small RNAs associated with Piwi

OSCs were treated with Imp α 3-siRNAs, or EGFP-siRNAs as a negative control, to knockdown *Impa3*. Myc-Piwi was then expressed in the cells, and immunoprecipitated using anti-myc monoclonal antibody as described above. After extensive washing, RNAs in the immunoprecipitated materials were isolated using Isogen (Sigma) and visualized by ³²P-labeling. Typhoon FLA 9500 (GE Healthcare) was used for the detection of RI signal.

Plasmid construction

I used plasmids pAcM-Piwi and pAcM-EGFP that were constructed and used previously (Saito et al. 2009) to express myc-Piwi and myc-EGFP in OSCs. To yield pAcF-Piwi for expressing flag-Piwi in OSCs and S2 cells, the region encoding a myc peptide in pAcM-Piwi was exchanged with a DNA fragment encoding a flag peptide using NEBuilder HiFi DNA Assembly Master Mix (NEB). The PCR primers used were F-Piwi-I-F/F-Piwi-I-R and F-Piwi-V-F/F-Piwi-V-R (Table 1). To express myc-*Impα1*, myc-*Impα2*, and myc-*Impα3* in OSCs, pAcM-*Impα1*, pAcM-*Impα2*, and pAcM-*Impα3* were produced by inserting each full-length *Impα* cDNA isolated from pGEX-*Impα1*, pGEX-*Impα2*, and pGEX-*Impα3* (see below) into a pAcM vector. To mutate the *Impα1*, *Impα2*, and *Impα3* cDNAs to be RNAi-resistant, PCRs were performed with PrimeSTAR Max (Clontech) using primers *Impα1*-F/*Impα1*-R, *Impα2*-F/*Impα2*-R, and *Impα3*-F/*Impα3*-R, respectively. To express myc-Mael-SV40-NLS, the region encoding 5xNLS was removed by PCR using PrimeSTAR Max from pAcM-Mael-SV40-6xNLS, which was a gift from K. Sato (University of Tokyo), and primers Mael-SN-F/Mael-SF-R. To yield pAcM-Piwi-N72-EGFP, a DNA fragment encoding Piwi-N72 was amplified by KOD plus neo DNA polymerase (Toyobo) using pAcM-Piwi as a template. The PCR fragment was inserted into pAcM-EGFP by

In-Fusion HD Cloning Kit (Takara), using primers PN72-I-F/PN72-I-R and PN72-V-F/PN72-V-R. To yield pAcM-Piwi-N20-EGFP, pAcM-Piwi-N34-EGFP, pAcM-Piwi-N36-EGFP, pAcM-Piwi-N54-EGFP and pAcM-Piwi-N(21-72)-EGFP, PCRs were performed using pAcM-Piwi-N72-EGFP as a template and primers PN20E-F/PN20E-R, PN34E-F/PN34E-R, PN36E-F/PN36E-R, PN54E-F/PN54E-R and PN(21-72)-F/PN(21-72)-R, respectively. pAcM-Piwi-N(7-34)-EGFP was produced from pAcM-Piwi-N34-EGFP using primers PN(7-34)-F/PN(7-34)-R. To yield pAcM-Piwi-NLS-M1, -M2, -M3, -M4, -M5, and - Δ N36, PCRs were performed with PrimeSTAR Max using pAcM-Piwi as a template and primers PN-M1-F/PN-M1-R, PN-M2-F/PN-M2-R, PN-M3-F/PN-M3-R, PN-M4-F/PN-M4-R, PN-M5-F/PN-M5-R, and PN Δ 36-F/ PN Δ 36-R, respectively. To yield pAcM-NP-NLS-EGFP, two oligos, NP-sense and NP-antisense, were annealed, digested with EcoRI and HindIII, and inserted into pAcM-EGFP. To yield pAcM-SV40-NLS-Piwi- Δ N, the cDNA encoding Piwi- Δ N was amplified by PCR using pAcM-Piwi as a template and primers SN-Piwi-F/SN-Piwi-R. Then, the PCR fragment was inserted into pAcM-SV40-NLS (see below) at the XhoI and MluI sites. To yield pAcM-SV40-NLS, two oligos, SV40-sense and SV40-antisense, were annealed, digested with EcoRI and HindIII, and inserted into a pAcM vector. To yield pAcM-Piwi-NLS-Piwi, the DNA fragment encoding

Piwi-NLS was amplified by PCR using pAcM-Piwi as a template. The PCR fragment was inserted into pAcM-Piwi by PCR using NEBuilder HiFi DNA Assembly Master Mix. The PCR primers used were PN36-I-F/PN36-I-R and PN36-V-F/PN36-V-R. To replace SSTs of Piwi-NLS to AAAA or DDDD to produce pAcM-Piwi-AAAAmut and pAcM-Piwi-DDDDmut, PCR was performed using the primers 4A-F/4A-R or 4D-F/4D-R respectively and the template was AcM-Piwi. To yield pGEX-*Impα1*, pGEX-*Impα2*, and pGEX-*Impα3* to produce GST-*Impα1*, GST-*Impα2*, and GST-*Impα3* in *E. coli*, full-length cDNAs of *Impα1*, *Impα2*, and *Impα3* were each inserted respectively into pGEX-5X-1 vectors (GE Healthcare). Full-length cDNA of each *Impα* was obtained by RT-PCR using total RNAs isolated from OSCs. For the RT-PCRs, ReverTra Ace (Toyobo) and KOD plus neo DNA polymerase were used with primers *Gimpα1*-F/*Gimpα1*-R, *Gimpα2*-F/*Gimpα2*-R, and *Gimpα3*-F/*Gimpα3*-R, respectively. To yield pAcM-Piwi- Δ N20-73 and - Δ N47-73, PCRs were performed using pAcM-Piwi as a template and KOD plus neo DNA polymerase. The PCR primers were PN Δ 20-73-F/PN Δ 20-73-R and PN Δ 47-73-F/PN Δ 47-73-R, respectively. To produce pAcM-Piwi- Δ N20 and pAcM-Piwi- Δ N47, the DNA fragments encoding Piwi- Δ N20 and Piwi- Δ N47 were amplified by PCR using pAcM-Piwi as a template with primers PN Δ 20-F/PN Δ 20-R and PN Δ 47-F/PN Δ 47-R, respectively, then treated with EcoRI and inserted into

a pAcM vector. To yield pGEX-Piwi-N72-120, pAcM-Piwi-N90-160 and pAcM-Piwi-N130-200, DNA fragments encoding Piwi-N75-100, Piwi-N100-150, and Piwi-N150-200 were amplified by PCR using pAcM-Piwi as a template with primers PN72-120-I-F/PN72-120-I-R, PN90-160-I-F/PN90-160-I-R, and PN130-200-I-F/PN130-200-I-R, then treated with EcoRI and NotI, and inserted into pGEX-5X-1. To yield pAc-Piwi expressing Piwi in S2 cells, the DNA fragment encoding a myc peptide was deleted from pAcM-Piwi by PCR using PrimeSTAR Max and primers AcP-F/AcP-R. To produce pAcM-Piwi-NLS-35linker-Piwi Δ N, 35 amino acids-linker was inserted into pAcM-Piwi by using NEBuilder HiFi DNA Assembly Master Mix. The sequence except linker was amplified by PCR using primers Link-F/Link-R. 35 amino acids-linker was produced by hybridizing sense oligonucleotides

TTCAGAGGATCTTCAGGTGGCGGAGGGAGCGGTGGCGGAGGGA
 GCGGTGGCGGAGGGAGCGGTGGCGGAGGGAGCGGTGGCGGAG
 GGAGCGGTGGCGGAGGGAGCGGTGGCGGAGGGAGCTCAGGTGA
 CCCGAGA and antisense oligonucleotides

TCTCGGGTCACCTGAGCTCCCTCCGCCACCGCTCCCTCCGCCACC
 GCTCCCTCCGCCACCGCTCCCTCCGCCACCGCTCCCTCCGCCACC
 GCTCCCTCCGCCACCGCTCCCTCCGCCACCTGAAGATCCTCTGAA.

These were purchased from Integrated DNA Technologies. All PCR primers used in this study were listed in Table1.

Results

Results

Antibody production

The full-length GST-Imp α 1, GST-Imp α 2 or GST-Imp α 3 was injected into mice three times (Figure 8A). After that, the reactivity of anti-serum of these mice was checked by western blotting using OSCs before and after each Imp α RNAi treatment. The serum used here was diluted to 1/2,000. Spleen and myeloma were fused to obtain hybridomas, which were proceeded to ELISA screening. The hybridomas showing the reactivity to Imp α 1, Imp α 2 or Imp α 3 were selected. Approximately one thousand wells were screened. The numbers of the wells that showed the reactivity were as follows; 58 for Imp α 1, 68 for Imp α 2 and 28 for Imp α 3 (Figure 9A, 9B and 9C). These cells were cultured further and the reactivity was checked again by western blotting. Finally, the numbers of each monoclonal antibody was as follows; 3 for Imp α 1, 2 for Imp α 2 and 2 for Imp α 3. After monoclonalization, clones that showed the reactivity for each Imp α were cultured in large-scale (Figure 9D, 9E and 9F).

The monoclonal antibody was checked the effect by western blotting using normal OSC or Imp α -depleted OSC to make sure the each siRNA and antibody effect. The siRNA sequence used here was shown in

Table 1. The antibodies produced in this study have the correct reactivity for each $Imp\alpha$ and siRNA was able to knock down each gene with low off-target effect by western blotting. The antibody was also immunoprecipitation and immunofluorescence whose results were former is shown here and latter is shown below, respectively (Figure 10 and 11C).

For $Imp\alpha1$, 8H1(IgG1) is applied for western blotting, 6H9(IgG2a) for immunoprecipitation and 7B7B9(IgM) for immunofluorescence. For $Imp\alpha2$, 9H2(IgG1) is applied for western blotting and immunofluorescence and 8G10(IgG2a) for immunoprecipitation. For $Imp\alpha3$, 1F8(IgG1) is applied for western blotting and 3F9(IgG2b) for western blotting, immunofluorescence and immunoprecipitation.

Quantification of $Imp\alpha1$, $Imp\alpha2$, $Imp\alpha3$ protein levels in OSC

Our previous RNA-sequencing data (Sumiyoshi et al. 2016) suggested that *Impa2* was relatively highly expressed in OSCs, accounting for 70.7% of the total *Impa* expression, while the expression level of *Impa1* was much lower (4.0%) (upper bar graph in Figure 12A). The expression level of *Impa3* was between those of *Impa2* and *Impa1* (25.3%). To

estimate the levels of the Imp α proteins (Figure 12B) by western blotting, we first produced monoclonal antibodies against each of the proteins as described above (Figure 8A, 11A and 11B). Comparison of the signals of the endogenous Imp α proteins in OSCs with those of recombinant Imp α proteins suggested that the ratio of abundance levels of Imp α 1, Imp α 2 and Imp α 3 proteins in OSCs was about 5:77.5:17.5 (lower bar graph in Figure 12A and Figure 12B). The corresponding monoclonal antibodies detected each Imp α protein in both the nucleus and the cytoplasm of OSCs in immunofluorescence analyses (Figure 11C).

Piwi mislocalized only in Imp α 2 or Imp α 3 depletion and the mislocalization was not affected for piRNA loading

Imp α 2 accounted for about 78% of total Imp α proteins in the OSCs (Figure 12A). Therefore, after depletion of Imp α 2, the amounts of Imp α 1 and Imp α 3 proteins in the OSCs may not be enough to import all cargos to the nucleus. Indeed, depletion of Imp α 2 greatly affected the cellular localization of Piwi (Figure 13B). However, after depletion of Imp α 3, the amount of Imp α 2 remained high in OSCs (Figure 11B); therefore, the finding that Piwi nuclear localization was affected by loss of

Imp α 3 (Figure 13C) was somewhat confusing.

Next, I checked the influence for piRNA loading by Imp α depletion. As a result, piRNA loading was not influenced by Imp α knock-down, which means that piRISC would form completely (Figure 15). Thus, piRISC could not import into the nucleus because the transport factor, Imp α , is not there very much.

All three Imp α individually rescued the Piwi mislocalization that was caused by Imp α 2 or Imp α 3 depletion in OSC

The simplest explanation for the strange localization of Piwi by Imp α depletion is that Piwi nuclear localization requires both Imp α 2 and Imp α 3 simultaneously. To test this hypothesis, I performed rescue experiments. First, Imp α 2- and Imp α 3-lacking OSCs were prepared, and then each *Imp α* gene was expressed by co-transfection with flag-Piwi in the cells. If both Imp α 2 and Imp α 3 were simultaneously required for Piwi nuclear localization, ectopic expression of *Imp α 3* in Imp α 2-lacking OSCs would not restore Piwi nuclear localization, while ectopic expression of *Imp α 2* should rescue the defective phenotype. Examination revealed that not only *Imp α 2* expression, but also *Imp α 1* and *Imp α 3* expression (all

Impα genes were RNAi-resistant) rectified Piwi nuclear localization (Figure 14A). Similarly, ectopic expression of all individual *Impα* genes rescued the defective phenotype caused by depletion of *Impα3* (Figure 14B). Therefore, the idea that *Impα2* and *Impα3* were simultaneously required for Piwi nuclear localization was excluded.

The nuclear localization of the cargo protein containing SV40-NLS was not affected by *Impα* depletion

An alternative explanation may be that the binding activity of Piwi-NLS to *Impα2* was relatively low and therefore *Impα2* prioritized cargos other than Piwi in nuclear import when the total amount of *Impα* proteins was reduced, albeit only by about 18%, as a consequence of, for instance, *Impα3* depletion. To check this, I examined whether the subcellular localization of SV40-NLS-cargo was affected by lack of *Impα3* as well as *Impα2*. To this end, Maelstrom (Mael) fused with a myc-tag and a monopartite SV40-NLS at the N- and C-terminal ends of Mael, respectively, was employed. Mael is one of the piRNA factors required in germ cells, but is dispensable for the somatic piRNA pathway in OSCs (Sienski et al. 2012; Matsumoto et al. 2015). I found that depletion of

neither Imp α 2 nor Imp α 3 affected cellular localization of myc-Mael-SV40-NLS (cargo-SV40-NLS in Figure 16), suggesting that efficiency of nuclear import of Piwi-NLS was somewhat lower than that of monopartite SV40-NLS.

Determination of Piwi-NLS

Previously, we showed that a Piwi mutant Piwi- Δ N that lacked 72 amino acid residues from the N-terminal end was mislocalized to the cytoplasm, although Piwi- Δ N formed piRISCs with piRNAs as well as wild-type Piwi (Saito et al. 2009). The 72 residues were very basic and arginine and lysine residues together accounted for 22.2% (17 out of 72 residues), which is a typical feature of classical NLSs bound with Imp α proteins (Figure 17A). We fused the peptide consisting of the 72 residues to EGFP and found that this fusion protein was localized exclusively to the nucleus (Figure 17B). However, the peptide was too long to be defined as a monopartite or bipartite NLS. Thus, I deleted 36 N-terminal residues from Piwi and examined the cellular localization. This mutant Piwi- Δ N36 localized almost exclusively in the cytoplasm (Figure 17C). I then fused the 36 residues to EGFP and found that this fusion protein, Piwi-N36-EGFP, strongly accumulated in the nucleus similar to Piwi-N72-EGFP (Figure

17B and 17C). In contrast, Piwi-N20-EGFP, which contained only 20 residues from the N-terminal end of Piwi was found to be throughout the cells, although the 20 residues included a basic stretch 7-RGRRR-11 (Figure 17C). Based on these results, I defined the 1-36 residues at the N-terminal end of Piwi as the Piwi-NLS.

To more strictly determine Piwi-NLS, Arg7-Arg34 of Piwi N-terminus was fused to EGFP (Figure 17D). As a result, this protein was also localized to the nucleus. This indicates that Met1-Gly6 and Gly35-Ser36 are unnecessary to be involved in Piwi-NLS. However it should be noted that, in this study, I performed the experiments using Met1-Ser36 as Piwi-NLS.

Piwi-NLS is a bipartite NLS

Next, I produced a series of Piwi-NLS mutants in the context of full-length Piwi. I first mutated four residues 9-RRRP-12 of Piwi to four alanine residues. This mutant Piwi-NLS-M1 appeared in the cytoplasm, similar to Piwi- Δ N (Saito et al. 2009) (Figure 18A). Piwi-NLS-M2, where Arg22 was mutated to alanine, was localized to the nucleus (Figure 18A), and Piwi-NLS-M3, where Arg34 was mutated to alanine, was found in both the nucleus and the cytoplasm. However, Piwi-NLS-M4 and

Piwi-NLS-M5, where Lys31 and Lys31/Arg34 were mutated to alanine residues, respectively, were not localized to the nucleus (Figure 18A). In summary, two small basic islands around 9-RRRP-12 and 31-KVFR-34 within the 36-residue Piwi-NLS sequence were necessary for Piwi nuclear localization. To strengthen the rightfulness of these phenomena, Piwi-N(21-72), which does not have 9-RRRP-12, fused EGFP. This mutant could not show complete nuclear localization, which is meant N-terminus would be needed to localize to the nucleus (Figure 18B). Thus, we defined Piwi-NLS as a bipartite NLS.

Cargo protein with Nucleoplasmin NLS (NP-NLS) behaved similarly to Piwi in $\text{Imp}\alpha$ -depleted OSCs

I then took NP-NLS, a representative of bipartite NLSs, and fused it to EGFP to produce NP-NLS-EGFP. NP-NLS-EGFP was localized exclusively to the nucleus of normal OSCs, as expected, but was detected in the cytoplasm under conditions where $\text{Imp}\alpha 2$ and $\text{Imp}\alpha 3$ had been depleted (NP-NLS-cargo in Figure 19A and 19B), similar to Piwi (Figure 13) but unlikely to SV40-NLS-containing cargo (Figure 16). These results suggest that the sensitivity that Piwi showed to a subtle reduction in the total amount of $\text{Imp}\alpha$ proteins in OSCs was not unique to Piwi and that

monopartite NLSs likely have higher efficiency in nuclear transport than bipartite NLSs, at least in OSCs.

‘Protein X’ may hide Piwi-NLS to prevent Imp α binding prior to Piwi-piRNA loading

Piwi nuclear localization requires not only its NLS but also piRNA loading, suggesting that Piwi-NLS is not accessible for Imp α in the cytosol until Piwi is loaded with piRNA. One hypothesis was that an unknown protein (temporally termed as protein X) occupied the NLS of piRNA-free Piwi, blocking Imp α binding to the NLS. Then, piRNA loading onto Piwi triggered displacement of the protein X from Piwi-NLS, allowing Piwi-piRISC to be successfully localized to the nucleus. To test this model, I exchanged Piwi-NLS with SV40-NLS to determine if the Piwi mutant SV40-NLS-Piwi- Δ N required piRNA loading or not to be localized to the nucleus. I assumed that SV40-NLS was not bound with protein X in OSCs based on the observation that cargo-SV40-NLS was successfully localized to the nucleus in OSCs (Figure 16). Therefore, protein X would not block the interaction of Imp α with SV40-NLS-Piwi- Δ N, and this fusion protein would be translocated to the nucleus without piRNA loading. However,

against my expectation, the mutant failed to be localized to the nucleus when piRNA biogenesis had been compromised by Yb depletion (Figure 18). Thus, the “protein X” hypothesis was excluded.

Addition of another Piwi-NLS leads Piwi to be localized to the nucleus in a piRNA-independent manner

An alternative model is that Piwi can hide its own NLS intramolecularly from Imp α until piRNA is loaded onto Piwi (Figure 25). To examine this possibility, I fused another Piwi-NLS composed of 36 residues to wild-type Piwi N-terminally. This process extended the NLS by duplication of the sequence in the context of full-length Piwi. If this additional Piwi-NLS projected into the cellular environment beyond the surface of piRNA-free Piwi, I considered Imp α would bind to it and translocate the mutant Piwi-NLS-Piwi to the nucleus, regardless of piRNA loading. Indeed, Piwi-NLS-Piwi was localized to the nucleus even after Yb depletion (Figure 21A). Addition to these experiments, I inserted the linker seven GGGGS repeats between Piwi-NLS and rest of Piwi, which is replaced second Piwi-NLS of Piwi-NLS-Piwi to the linker. This Piwi-NLS-35linker-Piwi Δ N mutant localized to the nucleus after Yb depletion (Figure 21B). Also, Piwi-NLS-M5 mutant, which localizes in cytosol completely,

is added Piwi-NLS. This Piwi-NLS-Piwi-NLS-M5 mutant showed nuclear localization piRNA-independently (Figure 21C). These results strongly support the idea that Piwi autoregulates its nuclear localization by a conformational change that switches the accessibility of the NLS to the cellular environment in a piRNA loading-dependent manner (Figure 21A). However, the underlying mechanism of this change remains to be determined.

A conformational change induced by piRNA loading might lead Piwi-NLS to be expose to Imp α

Human Ago2 (hAgo2) that was not bound with guide RNA was fragmented to domains in limited proteolysis assays, but guide RNA loading made hAgo2 resistant to the proteolysis treatment (Elkayam et al. 2012) (Figure 22A). I tested whether Piwi behaved similarly in the assays. To this end, I expressed Piwi in cultured *Drosophila* Schneider 2 (S2) cells, which are non-gonadal somatic cells, so do not operate the piRNA pathway. Indeed, Piwi expressed in S2 cells was devoid of piRNAs or any other RNAs, and was cytoplasmic (Figure 22B). I then immunopurified piRNA-free Piwi from S2 cells using anti-Piwi monoclonal antibody 3G11.

In parallel, Piwi-piRISC was immunopurified from OSCs using 3G11. The epitope of 3G11 was within the 20 residues at the N-terminal end that corresponded to the first half of the Piwi-NLS (Figure 23A). In accordance with this fact, I found that immunopurification of piRNA-free Piwi from S2 cells was much more difficult than immunopurification of Piwi-piRISC from OSCs, so to obtain comparable amounts of Piwi I prolonged the duration of immunoprecipitation from S2 cells. Also, the cell number of S2 cells used was doubled compared with that of OSCs. Both Piwi fractions were subjected to limited proteolysis assays. First, I used thermolysin because it was employed in the original hAgo2 study (Elkayam et al. 2012). However, even a low final thermolysin concentration of 0.08 ng/mL nearly completely degraded even Piwi-piRISC (data not shown). I then used chymotrypsin, which I found successfully released a large portion of Piwi-piRISC to the supernatant (Figure 22C), as was the case for Siwi-piRISC in our previous study (Matsumoto et al. 2016). The large portion of Piwi in the supernatant was detected by another anti-Piwi monoclonal antibody 4D2 (Saito et al. 2009) by western blotting. This phenomenon was also checked by making the same condition in OSC, which meant piRNA-free state was prepared by GasZ knockdown (Figure 22D). The epitope of 4D2 was determined to be located between Arg72 and Lys90 (Figure 23B), suggesting that the proteolysis occurred upstream of the 4D2 epitope. In contrast, for piRNA-free Piwi, multiple 4D2-positive

bands appeared exclusively in the bead fraction, implying that proteolysis occurred at multiple sites downstream of the 4D2 epitope. These results strongly suggest that the N-terminal region of approximately 200 residues of Piwi (including Piwi-NLS and 3G11/4D2 epitopes) was hardly accessible when Piwi was devoid of piRNAs, but piRNA loading induced a major conformational change in Piwi, as in hAgo2, exposing the N-terminal region to the environment.

Imp α and Piwi binding depends on piRNA binding of Piwi

To analyze whether Piwi binds Imp α , immunoprecipitation using anti-flag antibody and western blotting were performed. I found that Piwi bound Imp α 2 or Imp α 3 when it formed piRISC with piRNA-free Piwi with Imp α 2 or Imp α 3 was very low (Figures 23C and 23D). This strengthened our original idea that Piwi bound with Imp α only after Piwi-NLS was exposed to the environment upon piRISC formation with piRNAs. I also performed the binding assay between Imp α 3 and Piwi-NLS-M1 or Piwi-NLS-M5 shown in Figure 18A. Both Piwi mutants showed attenuated binding activity (Figure 23E). These results agreed with the results shown in Figure 18A. I concluded that the ‘bipartite’ Piwi-NLS is the binding

region of Piwi with Imp α .

sDMA modification and phosphorylation of Piwi have little impact on Piwi nuclear localization

To test the possibility that post-translational modification of Piwi affects Piwi nuclear localization, I examined if Piwi-NLS is modified with symmetric dimethylarginine (sDMA) and phosphorylation. The former was checked by western blotting using a specific antibody against sDMA modification (SYM11). Siwi, a silkworm PIWI protein expressed in cultured ovarian germ cells termed BmN4 cells was sDMA-modified, which was shown to be required for associating with a Tudor domain containing protein PAPI (Nishida et al. 2018) (Figure 24A). However, Piwi in OSCs was undetected with SYM11 (Figure 24A), suggesting that Piwi is not sDMA-modified in the cells, unlike Siwi in BmN4 cells.

Piwi contains a SSTS (Ser-Ser-Thu-Ser) peptide at the N terminal region (Figure 24B). I speculated that one or more amino acids in the SSTS sequence may be phosphorylated in OSCs and that the post-translational modification may affect Piwi nuclear localization. To test the possibility, I mutated the SSTS sequence to AAAA and DDDD in Piwi full length context (Figure 24B) and checked the cellular localization of the mutants.

Both mutants were localized to the nucleus as well as wild-type Piwi protein (Figure 24C). These results suggest that, although I still do not know if Piwi is phosphorylated at the peptide region or not, such post-translational modification may be unnecessary for, and disturb, Piwi nuclear localization.

Discussion

Discussion

***Drosophila* Imp α monoclonal antibodies**

To analysis Piwi nuclear transport by biochemical assay, anti-Imp α antibodies would help me carrying out my task. Although some laboratories in USA, United Kingdom or Austria had produced polyclonal antibody of *Drosophila* Imp α , no monoclonal antibodies were exiting. Then, Imp α 1 and Imp α 2 polyclonal antibodies were kindly gifted from Sue Cotterill (University of London). However, these antibodies did not react correctly, which means that they reacted all kinds of Imp α proteins. Fortunately, my laboratory has the technology to produce monoclonal antibodies. Therefore, I could produce high-quality antibodies of each Imp α with help from Dr. Nishida, the assistant professor here. The antibodies against each Imp α were applied for western blotting, immunofluorescence and immunoprecipitation. However, other experiments such as Chip, CLIP or FACS were not checked because they do not need for this study.

Imp α is a nuclear import factor of Piwi

In this study, I revealed that Imp α played a vital role in Piwi nuclear localization in OSCs and that Piwi autoregulated its cellular localization by controlling the accessibility of its own N-terminal bipartite NLS to Imp α , by changing the structure in a piRNA loading-dependent manner. With this “layered” regulation, Piwi was strictly localized to the cytoplasm before piRNA loading. However, once piRNA was loaded onto Piwi, Piwi-NLS was exposed to the cellular environment, where the adaptor protein Imp α bound to it and triggered the nuclear import of Piwi-piRISC together with Imp β . Unfortunately, depletion of Imp β in OSCs by RNAi caused severe damage to the cells; thus, the necessity of Imp β in the processing remains unclear.

Piwi may change its conformation whether piRNA is loaded or not

The limited proteolysis analysis provided compelling evidence that Piwi drastically changed the conformation in a piRNA-dependent manner, similar to what was reported for hAgo2. However, direct evidence is still missing. For this, crystal structural analysis of Piwi in the presence and

absence of piRNAs is desirable. However, I currently face a huge problem, because purifying a large amount of recombinant PIWI proteins without piRNAs is a nightmare due to their high instability in cellular environments. However, we recently solved the crystal structure of Siwi-piRISC (Matsumoto et al. 2016). To make the crystals, endogenous Siwi-piRISC was immunisolated from cultured BmN4 cells using anti-Siwi antibody. Because the vast majority of Siwi in BmN4 cells are loaded with piRNAs and the interaction between them is so tight, removing piRNAs from the piRISCs was the issue to be solved. Using a powerful electron-cryo-microscopy may be another way to go; however, the molecular weight of PIWI proteins is around 90-100 kDa, which may be too small for this type of analysis. I am currently exploring gentle but efficient ways of removing piRNAs from PIWI-piRISCs.

Cargos often require a specific Imp α , but Piwi does not

Our rescue experiments revealed that all three Imp α proteins could individually rescue mislocalization of Piwi to the cytoplasm caused by loss of Imp α 2 and Imp α 3 in OSCs. This clearly excludes a paralog-specific role of Imp α in Piwi nuclear localization. However, previous genetic studies showed that sterility caused by *Imp α 2* mutations was not rescued by

ectopic expression of *Impα1* nor *Impα3*, although the levels of *Impα* mRNAs (and *Impα* proteins) ectopically expressed in the mutant ovaries were comparable to endogenous ones (Mason et al. 2002). Embryonic lethality of *Impα3* mutants was also not rescued by overexpression of *Impα1* or *Impα2* (Mason et al. 2003). These results suggest that some cargo proteins, crucial for gonadal development and fertility in *Drosophila*, were forced to remain cytoplasmic under the circumstance where other *Impα* isoforms were expressed in the mutant ovaries. Identification of cargos for which nuclear import is tightly controlled by a particular *Impα* protein is awaited.

Why does Piwi have a bipartite NLS?

Piwi bears a *bona fide* bipartite NLS. Why a bipartite, not monopartite, NLS evolved in Piwi is still unknown. My results revealed that bipartite NLSs, from both Piwi and NP showed less efficiency in nuclear import than monopartite NLSs, at least in OSCs. Therefore, it might be expected that having a monopartite NLS would simply be more effective and secure for exerting Piwi function in the nucleus. However, interestingly our results also showed that Piwi containing its own NLS was clearly more sensitive to loss of piRNA than Piwi bearing SV40-NLS

instead of its own NLS. This result suggests that Piwi autoregulation may be more controllable with bipartite NLSs than with monopartite NLSs, and this is most likely is the reason why Piwi evolutionally acquired a bipartite NLS rather than a monopartite NLS. Notably, the N-terminal sequence of MIWI2, one of three PIWI proteins expressed in mouse testis whose nuclear localization and subsequent piRNA-mediated transposon silencing in the nucleus also requires piRNA loading (Carmell et al. 2007; Siomi et al. 2011), is high similar to the N-terminal sequence of Piwi, including the NLS. It is likely that MIWI2 also evolutionally acquired a bipartite NLS rather than a monopartite NLS (Figure 26).

Conclusion

Conclusion

I identified Imp α as a novel nuclear import factor of Piwi and also understood Piwi had a bipartite NLS. Moreover, my results suggest that Piwi's conformational change occurs whether Piwi loads piRNA or not.

I concluded my research and understood the phenomenon described above. However, to understand more deeply, I would like to propose following contents for the next step of this study.

One is about Imp α . In OSC, the behavior of monopartite NLS and bipartite NLS are different. The monopartite NLS SV40-NLS is not influenced by depletion of the only one kind of Imp α . On the other hand, Piwi and the bipartite NLS Nucleoplasmin NLS are drastically influenced. These results means Imp α may prioritize the protein import having a monopartite NLS. Therefore, next step is to analyze whether the priority exists or not and whether Imp α prefers monopartite NLS to bipartite NLS by *in vitro* assay using purified proteins that have already prepared.

The other is about the conformational change of Piwi. The result that suggests Piwi conformation is changed if it does not form piRISC is shown in this study. To know more profound about this, I would like to solve the structure of Piwi. As discussed above, our lab with Nureki lab (Univ. of Tokyo) solved the structure of Siwi, which is a PIWI protein of *Bombyx mori*. This is the first report to solve the PIWI structure. However

as described above, this solved structure is in the condition binding with piRNA and its N-terminus is cut by nuclease. This means I could not know how the most N-terminus side was. Therefore, I would like to solve the structure of Piwi that is not having piRNA, piRNA-free Piwi. This may be the most difficult task throughout the world because to get piRNA-free Piwi *in vitro* is quite difficult. Now, I consider to start from piRISC because piRISC is stable and we will get easier than piRNA-free state. Then, piRNA will be degraded by RNase to get piRNA-free Piwi.

There are many phases in Piwi transposon silencing such as piRNA precursor transcription, piRNA maturation, piRISC behavior in nucleus and so on. However, for me, the most important thing is the step to go to the nucleus because piRISC acts there. To complete the research of Piwi nuclear import and its regulatory mechanism ultimately means to save us infertility and survive the species on the earth. I believe I could contribute and be a part of it.

References

References

Aravin AA, Hannon GJ, Brennecke J. 2007. The Piwi-piRNA pathway provides an adaptive defense in the transposon arm race. *Science* **318**: 761-764.

Brennecke J, Aravin AA, Stark A, Dus M, Kellis M, Sachidanandam R, Hannon GJ. 2007. Discrete small RNA-generating loci as master regulators of transposon activity in *Drosophila*. *Cell* **128**: 1089-1103.

Carmell MA, Girard A, Kant HJG, Bourc'his D, Bestor TH, Rooij DG, Hannon GJ. 2007. MIWI2 is essential for spermatogenesis and repression of transposons in the mouse male germline. *Dev Cell* **12**: 503-514.

Conti E, Uy M, Leighton L, Blobel G, Kuriyan J. 1998. Crystallographic analysis of the recognition of a nuclear localization signal by the nuclear import factor Karyopherin α . *Cell* **94**: 193-204.

Cox DN, Chao A, Baker J, Chang L, Qiao D, Lin H. 1998. A novel class of evolutionarily conserved genes defined by *piwi* are essential for stem cell self-renewal. *Genes Dev* **12**: 3715-3727.

Czech B, Preall JB, McGinn J, Hannon GJ. 2013. A transcriptome-wide RNAi screen in the *Drosophila* ovary reveals factors of the germline piRNA pathway. *Mol Cell* **50**: 749-761.

Dönertas D, Sienski G, Brennecke J. 2013. *Drosophila* Gtsf1 is an essential component of the Piwi-mediated transcriptional silencing complex. *Genes Dev* **27**: 1693-1705.

Elkayam E, Kuhn C-D, Tocilj A, Haase AD, Greene EM, Hannon GJ, Joshua-Tor L. 2012. The structure of human Argonaute-2 in complex with miR-20a. *Cell* **150**: 100-110.

Eulalio A, Huntzinger E, Izaurralde E. 2008. GW182 Interaction with Argonaute Is Essential for miRNA-Mediated Translational Repression and mRNA Decay. *Nat Struct Mol Biol* **15**: 346–353.

Fontes MR, Teh T, Toth G, John A, Pavo I, Jans DA, Kobe B. 2003. Role of flanking sequences and phosphorylation in the recognition of the simian-virus-40 large T-antigen nuclear localization sequences by importin-alpha. *Biochem J* **375**: 339-349.

Ghildiyal M, Zamore PD. 2009. Small silencing RNAs: an expanding universe. *Nat Rev Genetics* **10**: 94-108.

Girard A, Sachidanandam R, Hannon GJ and Carmell MA. 2006. A germline-specific class of small RNAs binds mammalian Piwi proteins. *Nature* **442**: 199-202.

Goldfarb DS, Corbett AH, Mason DA, Harreman MT, Adam SA. 2004. Importina: a multipurpose nuclear-transport receptor. *Trends Cell Biol* **14**: 505-514.

Görlich D, Prehn S, Laskey RA and Hartmann E. 1994. Isolation of a protein that is essential for the first step of nuclear protein import. *Cell* **79**: 767-778.

Görlich D. Transport into and out of the cell nucleus. 1998. *EMBO J* **17**: 2721-2727.

Grimson A, Srivastava M, Fahey B, Woodcroft BJ, Chiang HR, King N, Degan BM, Rokhsar DS, Bartel DP. 2008. Early origins and evolution of microRNAs and PIWI-interacting RNAs in animals. *Nature* **455**: 1193-1197.

Gunawardane LS, Saito K, Nishida KM, Miyoshi K, Kawamura Y, Nagami T, Siomi H, Siomi MC. 2007. A slicer-mediated mechanism for repeat-associated siRNA 5' end formation in *Drosophila*. *Science* **315**: 1587-1590.

Handler D, Meixner K, Pizka M, Lauss K, Schmied C, Gruber FS, Brennecke J. 2013. The genetic makeup of the *Drosophila* piRNA pathway. *Mol Cell* **50**: 762-777.

Ishizu H, Siomi H, Siomi MC. 2012. Biology of PIWI-interacting RNAs: new insights into biogenesis and function inside and outside of germlines. *Genes Dev* **26**: 2361-2373.

Iwasaki S, Kawamata T, Tomari Y. 2009. *Drosophila* Argonaute1 and Argonaute2 Employ Distinct Mechanisms for Translational Repression. *Mol Cell* **34**: 58-67.

Iwasaki YW, Siomi MC, Siomi H. 2015. PIWI-interacting RNA: Its biogenesis and functions. *Annu Rev Biochem* **84**: 405-433.

Iwasaki YW, Murano K, Ishizu H, Shibuya A, Iyoda Y, Siomi MC, Siomi H, Saito K. 2016. Piwi modulates chromatin accessibility by regulating multiple factors including histone H1 to repress transposons. *Mol Cell* **63**: 408-419.

Juliano C, Wang J, Lin H. 2011. Uniting germline and stem cells: the function of Piwi proteins and the piRNA pathway in diverse organisms. *Annu Rev Genet* **45**: 447-469.

Kalderon D, Richardson WD, Markham AF, Smith AE. 1984. Sequence requirements for nuclear location of simian virus 40 large-T antigen. *Nature* **311**: 33-38.

Kalmykova AI, Nurminsky DI, Ryzhov DV, Shevelyov YY. 2005. Regulated chromatin domain comprising cluster of co-expressed genes in *Drosophila melanogaster*. *Nucleic Acids Res* **33**: 1435-1444.

Kawamura Y, Saito K, Kin T, Ono Y, Asai K, Sunohara T, Okada TN, Siomi MC, Siomi H. 2008. *Drosophila* endogenous small RNAs bind to Argonaute 2 in somatic cells. *Nature* **453**: 793-797.

Khurana JS, Theurkauf W. 2010. piRNAs, transposon silencing, and *Drosophila* germline development. *J Cell Biol* **191**: 905-913.

Klenov MS, Sokolova OA, Yakushev EY, Stolyarenko AD, Mikhaleva EA,

Lavrov SA, Gvozdev VA. 2011. Separation of stem cell maintenance and transposon silencing functions of Piwi protein. *Proc Natl Acad Sci USA* **108**: 18760-18765.

Kobe B. 1999. Autoinhibition by an internal nuclear localization signal revealed by the crystal structure of mammalian importin α . *Nat Struct Mol Biol* **6**: 388-397.

Kussel P, Frasch M. 1995. Pendulin, a *Drosophila* protein with cell cycle-dependent nuclear localization, is required for normal cell proliferation. *J Cell Biol* **129**: 1491-1507.

Le Thomas A, Rogers AK, Webster A, Marinov GK, Liao SE, Perkins EM, Hur JK, Aravin AA, Tóth KF. 2013. Piwi induces piRNA-guided transcriptional silencing and establishment of a repressive chromatin state. *Genes Dev* **27**: 390-399.

Li C, Vagin VV, Lee S, Xu J, Ma S, Xi H, Seitz H, Horwich MD, Syrzycka M, Honda BM, Kittler EL, Zapp ML, Klattenhoff C, Schulz N, Theukauf WE, Weng Z, Zamore PD. 2009. Collapse of germline piRNAs in the absence of Argonaute3 reveals somatic piRNAs in flies. *Cell* **137**: 509-521.

Lippai M, Tilian L, Baros I, Mihaly J, Erdelyi M, Beleczi I, Mathe E, Posfai J, Nagy A, Udvardy A, et al. 2000. The *Ketel* gene encodes a *Drosophila* homologue of importin- β . *Genetics*. **156**: 1889-1900.

Livak KJ. 1990. Detailed structure of the *Drosophila melanogaster stellate* genes and their transcripts. *Genetics* **124**: 303-316.

Malone CD, Hannon GJ. 2009. Small RNAs as guardians of the genome. *Cell* **136**: 656-668.

Malone CD, Brennecke J, Dus M, Stark A, McCombie WR, Sachidanandam R, Hannon GJ. 2009. Specialized piRNA Pathways Act in Germline and Somatic Tissues of the *Drosophila* Ovary. *Cell* **137**: 522–535.

Mason DM, Fleming RJ, Goldfarb DS. 2002. *Drosophila melanogaster* importin $\alpha 1$ and $\alpha 3$ can replace importin $\alpha 2$ during spermatogenesis but not oogenesis. *Genetics* **161**: 157-170.

Mason DM, Mathe E, Fleming RJ, Goldfarb DS. 2003. The *Drosophila melanogaster* importin $\alpha 3$ locus encodes an essential gene required for the development of both larval and adult tissues. *Genetics* **165**: 1943-1958.

Mason DM, Stage DE, Goldfarb DS. 2009. Evolution of the metazoan-specific importin α gene family. *J Mol Evol* **68**: 351-365.

Matsumoto N, Sato K, Nishimasu H, Namba Y, Miyakubi K, Dohmae N, Ishitani R, Siomi H, Siomi MC, Nureki O. 2015. Crystal structure and activity of the endoribonuclease domain of the piRNA pathway factor Maelstrom. *Cell Rep* **11**: 366-375.

Matsumoto N, Nishimasu H, Sakakibara K, Nishida KM, Hirano T, Ishitani R, Siomi H, Siomi MC, Nureki O. 2016. Crystal structure of silkworm PIWI-clade Argonaute Siwi bound to piRNA. *Cell* **167**: 484-497.

Miyoshi K, Tsukumo H, Nagami T, Siomi H, Siomi MC. 2005. Slicer function of *Drosophila* Argonautes and its involvement in RISC formation. *Genes Dev* **19**: 2837-2848.

Muerdter F, Guzzardo PF, Gillis J, Luo Y, Yu Y, Chen C, Fekete R, Hannon GJ. 2013. A genome-wide RNAi screen draws a genetic framework for transposon control and primary piRNA biogenesis in *Drosophila*. *Mol Cell* **50**: 736-748.

Murota Y, Ishizu H, Nakagawa S, Iwasaki YW, Shibata S, Kamatani MK, Saito K, Okano H, Siomi H, Siomi MC. 2014. Yb integrates piRNA intermediates and processing factors into perinuclear bodies to enhance piRISC assembly. *Cell Rep* **8**: 103-113.

Nagao A, Sato K, Nishida KM, Siomi H, Siomi MC. 2010. Gender-specific hierarchy in nuage localization of PIWI-interacting RNA factors in *Drosophila*. *Front Genet* **2**: 1-9.

Nishida KM, Saito K, Mori T, Kawamura Y, Nagami-Okada T, Inagaki S, Siomi H, Siomi MC. 2007. Gene silencing mechanisms mediated by Aubergine-piRNA complexes in *Drosophila* male gonad. *RNA* **13**: 1911-1922.

Nishida KM, Iwasaki YW, Murota Y, Nagao A, Mannen T, Kato Y, Siomi H, Siomi MC. 2015. Respective functions of two distinct Siwi complexes assembled during PIWI-interacting RNA biogenesis in *Bombyx* germ cells. *Cell Rep* **10**: 193-203.

Nishida KM, Sakakibara K, Iwasaki YW, Yamada H, Murakami R, Kawamura T, Komada T, Siomi H, Siomi MC. 2018. Hierarchical roles of mitochondrial Papi and Zucchini in *Bombyx* germline piRNA biogenesis. *Nature* **555**: 260-264.

Ohtani H, Iwasaki YW, Shibuya A, Siomi H, Siomi MC, Saito, K. 2013. DmGTSF1 is necessary for Piwi-piRISC-mediated transcriptional transposon silencing in the *Drosophila* ovary. *Genes Dev* **27**: 1656-1661.

Olivieri D, Sykora MM, Sachidanandam R, Mechtler K, Brennecke J. 2010. An in vivo RNAi assay identifies major genetic and cellular requirements for primary piRNA biogenesis in *Drosophila*. *EMBO J* **29**: 3301-3317.

Phadnis N, Hsieh E, Malik HS. 2011. Birth, death, and replacement of karyopherins in *Drosophila*. *Mol Biol Evol* **5**: 1429-1440.

Pumroy RA, Cingolani G. 2015. Diversification of importin- α isoforms in cellular trafficking and disease states. *Biochem J* **466**: 13-28.

Ratan R, Mason DA, Sinnot B, Goldfarb DS, Fleming RJ. 2008. *Drosophila* importin $\alpha 1$ performs paralog-specific functions essential for gametogenesis. *Genetics* **178**: 839-350.

Riggleman B, Wieschaus E, Schedl P. 1989. Molecular analysis of the armadillo locus: uniformly distributed transcripts and a protein with novel internal repeats are associated with a *Drosophila* segment polarity gene. *Genes Dev* **3**: 96-113.

Robbins J, Dilworth SM, Laskey RA, Dingwall, C. 1991. Two interdependent basic domains in nucleoplasmin nuclear targeting sequence: identification of a class of bipartite nuclear targeting sequence. *Cell* **64**: 615-623.

Saito K, Nishida KM, Mori T, Kawamura Y, Miyoshi K, Nagami T, Siomi H, Siomi MC. 2006. Specific association of Piwi with rasiRNAs derived from retrotransposon and heterochromatic regions in the *Drosophila* genome. *Genes Dev* **20**: 2214-2222.

Saito K, Inagaki S, Mituyama T, Kawamura Y, Ono Y, Sakota E, Kotani H, Asai K, Siomi H, Siomi MC. 2009. A regulatory circuit for *piwi* by the large Maf gene *traffic jam* in *Drosophila*. *Nature* **461**: 1296-1301.

Saito K, Ishizu H, Komai M, Kotani H, Kawamura Y, Nishida KM, Siomi H, Siomi MC. 2010. Roles for the Yb body components Armitage and Yb in primary piRNA biogenesis in *Drosophila*. *Genes Dev* **24**: 2493-2498.

Sato K, Iwasaki YW, Shibuya A, Carninci P, Tsuchizawa Y, Ishizu H, Siomi MC, Siomi H. 2015. Krimper enforces an antisense bias on piRNA pools by binding AGO3 in the *Drosophila* germline. *Mol Cell* **59**: 553-563.

Schmidt A, Palumbo G, Bozzetti MP, Tritto P, Pimpinelli S, Schäfer U. 1999. Genetic and molecular characterization of *sting*, a gene involved in crystal formation and meiotic drive in the male germ line of *Drosophila melanogaster*. *Genetics* **151**: 749-760.

Sienski G, Dönertas D, Brennecke J. 2012. Transcriptional silencing of

transposons by Piwi and Maelstrom and its impact on chromatin state and gene expression. *Cell* **151**: 964-980.

Sienski G, Batki J, Senti KA, Dönertas D, Tirian L, Meixner K, Brennecke J. 2015. Silencio/CG9754 connects the Piwi-piRNA complex to the cellular heterochromatin machinery. *Genes Dev* **29**: 2258-2271.

Siomi MC, Sato K, Pezic C, Aravin AA. 2011. PIWI-interacting small RNAs: the vanguard of genome defence. *Nat Rev Mol Cell Biol* **12**: 246-258.

Stewart M. 2007. Molecular mechanism of the nuclear protein import cycle. *Nat Rev Mol Cell Biol* **8**: 195-208.

Sumiyoshi T, Sato K, Yamamoto H, Iwasaki YW, Siomi H, Siomi MC. 2016. Loss of *l(3)mbt* leads to acquisition of the ping-pong cycle in *Drosophila* ovarian somatic cells. *Genes Dev* **30**: 1617-1622.

Török I, Strand D, Schmitt R, Tick G, Török T, Kiss I, Mechler B. 1995. The overgrown hematopoietic organs-31 tumor suppressor gene of *Drosophila* encodes an Importin-like protein accumulating in the nucleus at the onset of mitosis. *J Cell Biol* **129**: 1473-1489.

Vagin VV, Sigova A, Li C, Seitz H, Gvozdev V, Zamore PD. 2006. A Distinct Small RNA Pathway Silences Selfish Genetic Elements in the Germline. *Science* **313**: 320–324.

Watanabe T, Totoki Y, Toyoda A, Kaneda M, Kuramochi-Miyagawa S, Obata Y, Chiba H, Kohara Y, Kono T, Nakano T, et al. 2008. Endogenous

siRNAs from Naturally Formed dsRNAs Regulate Transcripts in Mouse Oocytes. *Nature* **453**: 539–543.

Yamashiro H, Siomi MC. 2018. Piwi-interacting RNA in *Drosophila*: Biogenesis, Transposon Regulation, and Beyond. *Chem. Rev.* **118**: 4404-4421.

Yu Y, Gu J, Jin Y, Luo Y, Preall JB, Ma J, Czech B, Hannon GJ. 2015. Panoramix enforces piRNA-dependent cotranscriptional silencing. *Science* **350**: 339-342.

Figures

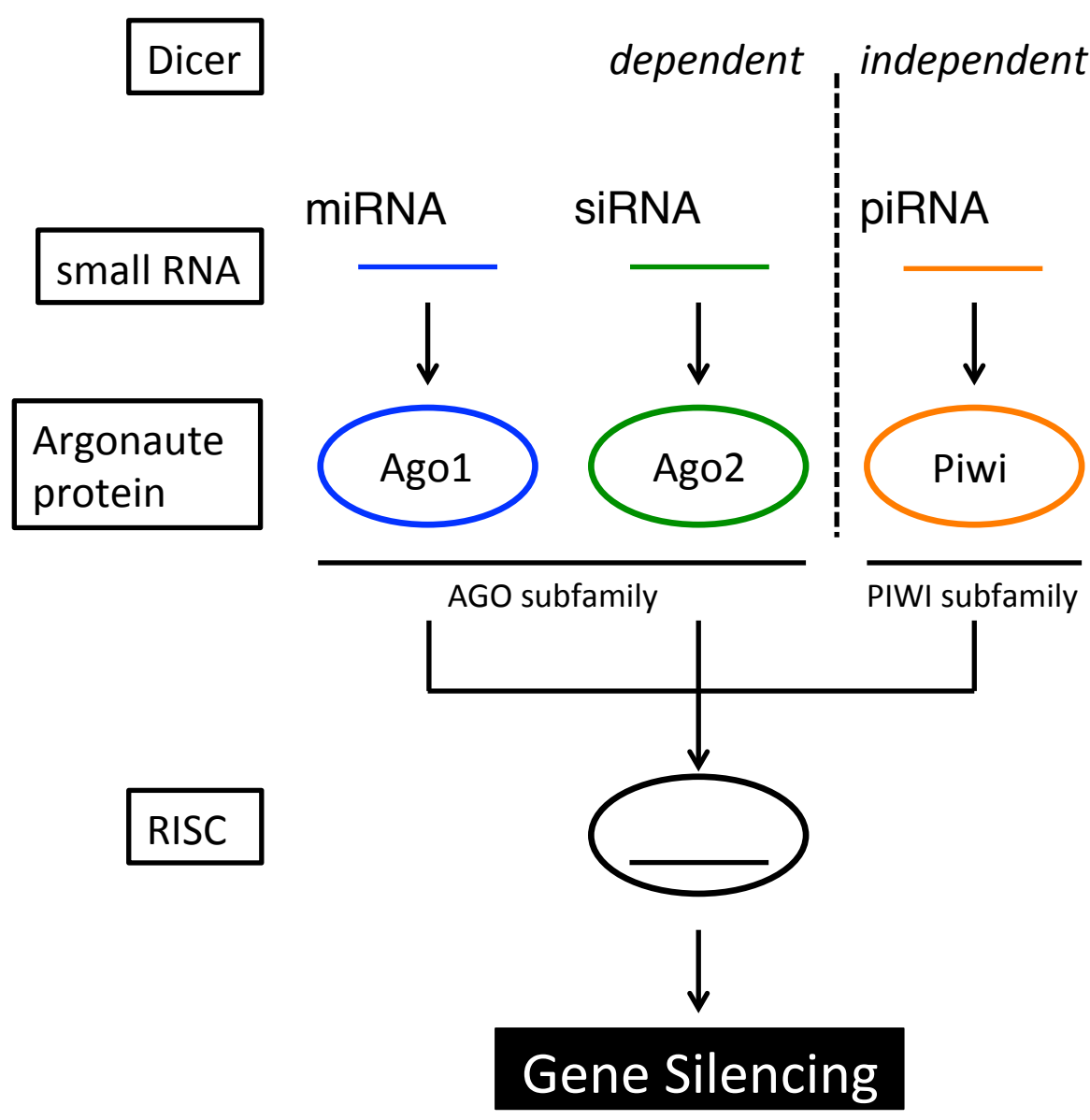


Figure 1. Gene silencing by PIWI subfamily proteins
 Each PIWI subfamily protein forms different RISC. However, the result, which small RNAs silences their target genes by their complementarity, is the same for every proteins.

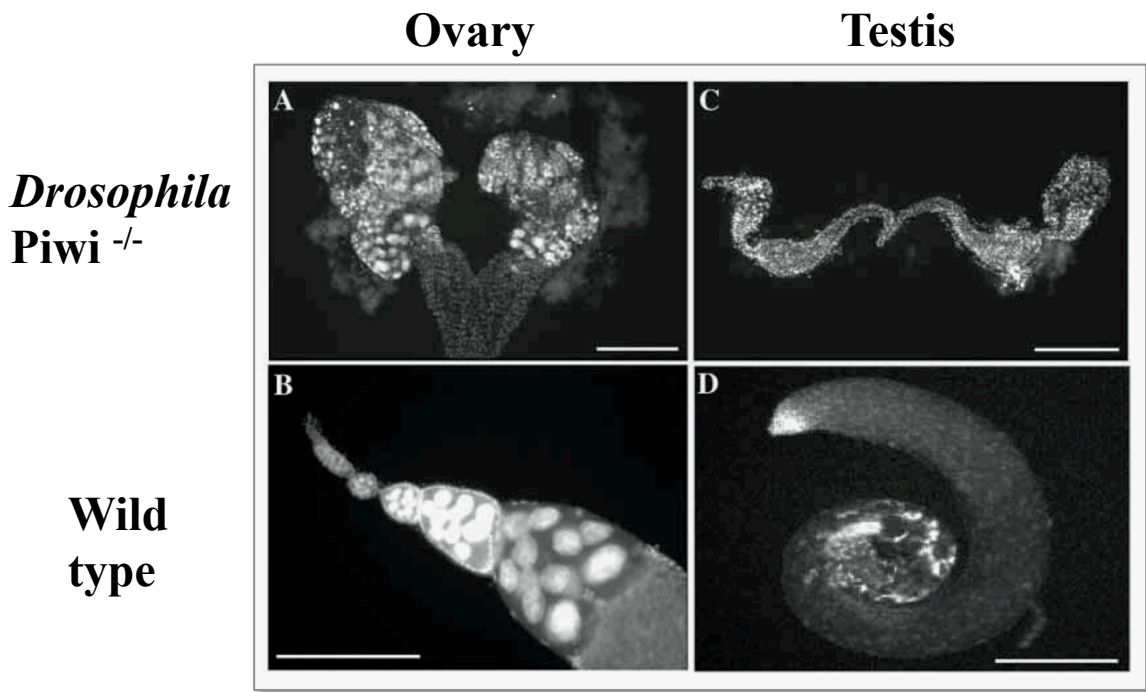


Figure 2. Loss-of-function of Piwi defects gametogenesis and infertility

The figure was modified from Cox *et al*, 2000. Loss-of-function of Piwi leads to hypoplasia of germlines and to be infertility.

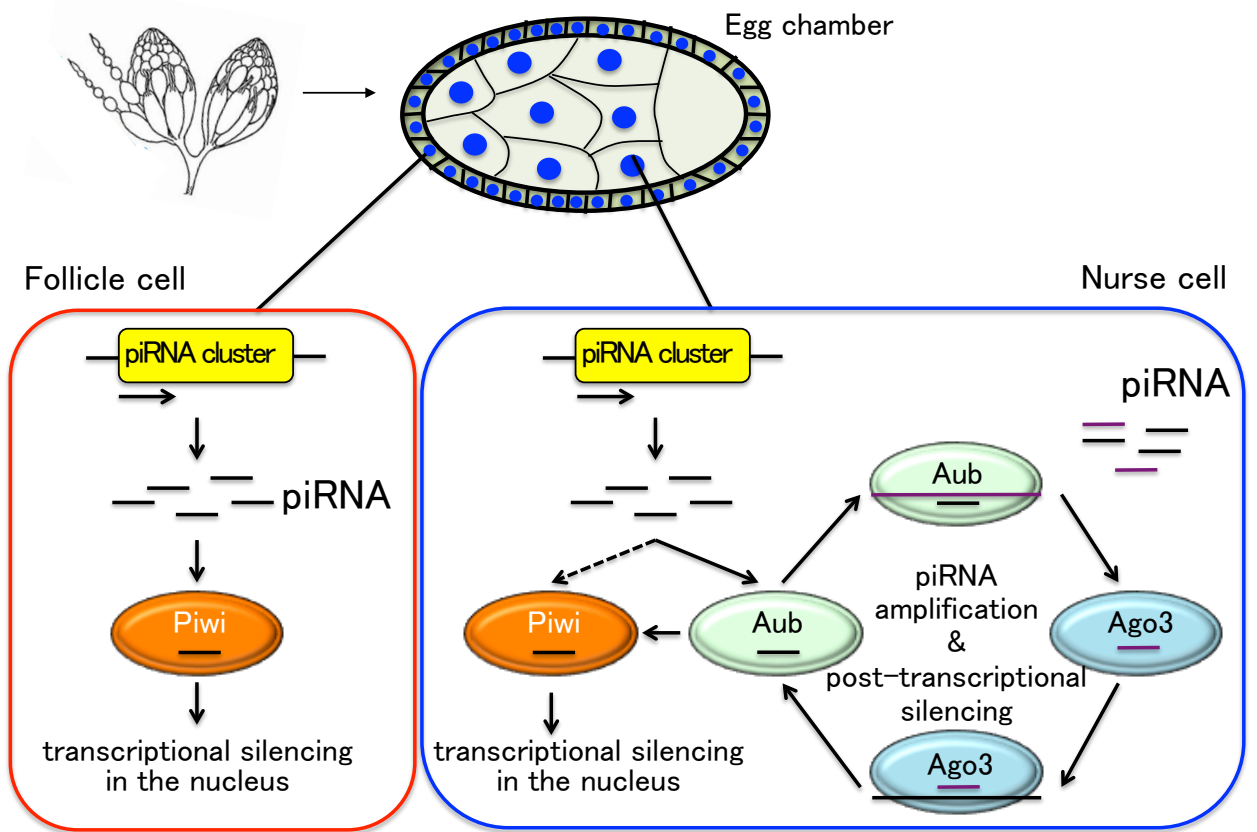


Figure 3. The role of PIWI proteins expressed in *Drosophila* ovary

Follicle cell only expresses Piwi and the pathway operated by Piwi is called primary pathway. Nurse cell expresses Piwi, Aub and Ago3 and both primary and secondary pathways functions.

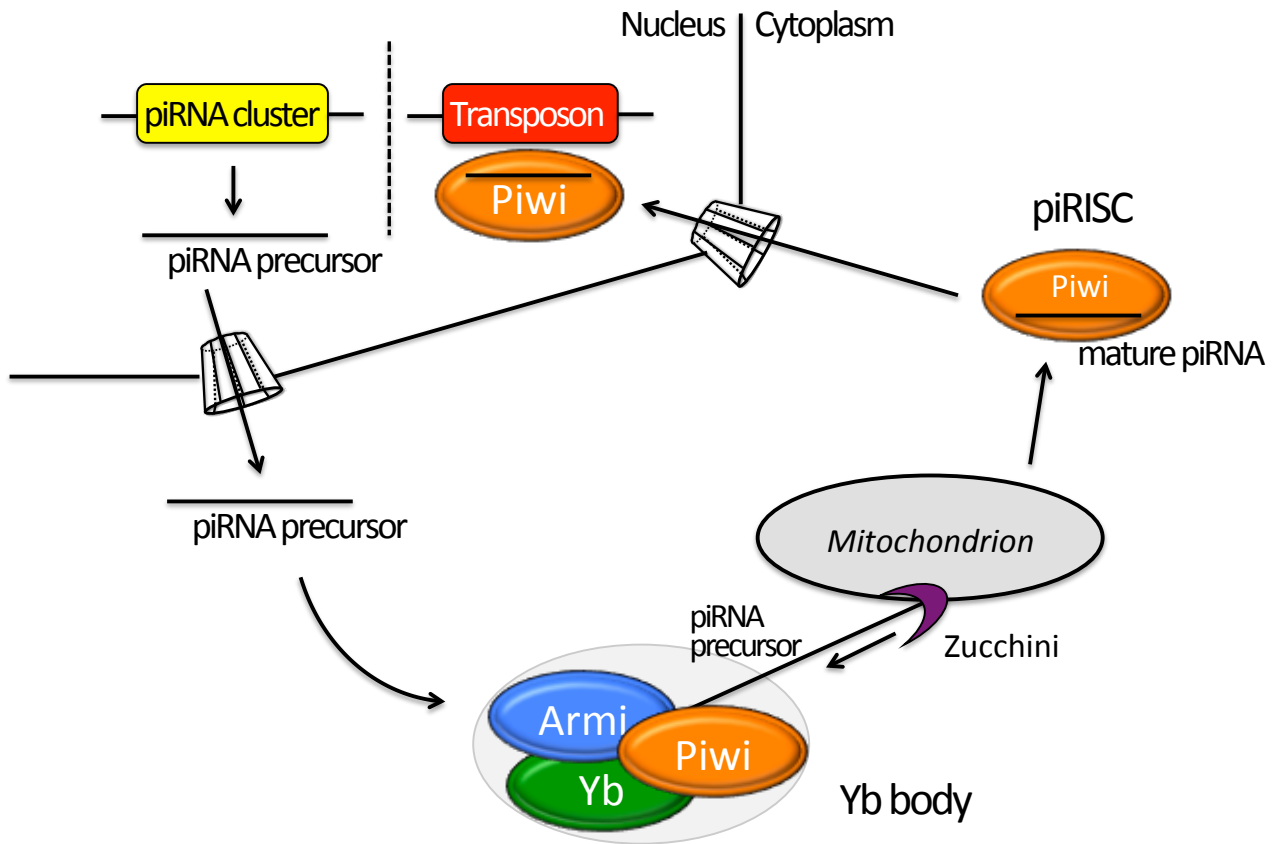


Figure 4. Primary pathway of transposon silencing operated by Piwi

A piRNA precursor is transcribed from piRNA cluster located in genome. It exports to cytoplasm and some processing make it to mature phase. Mature piRNA binds to Piwi and goes to nucleus. Then, to add H3K9me3 leads to heterochromatinization and complete silencing system.

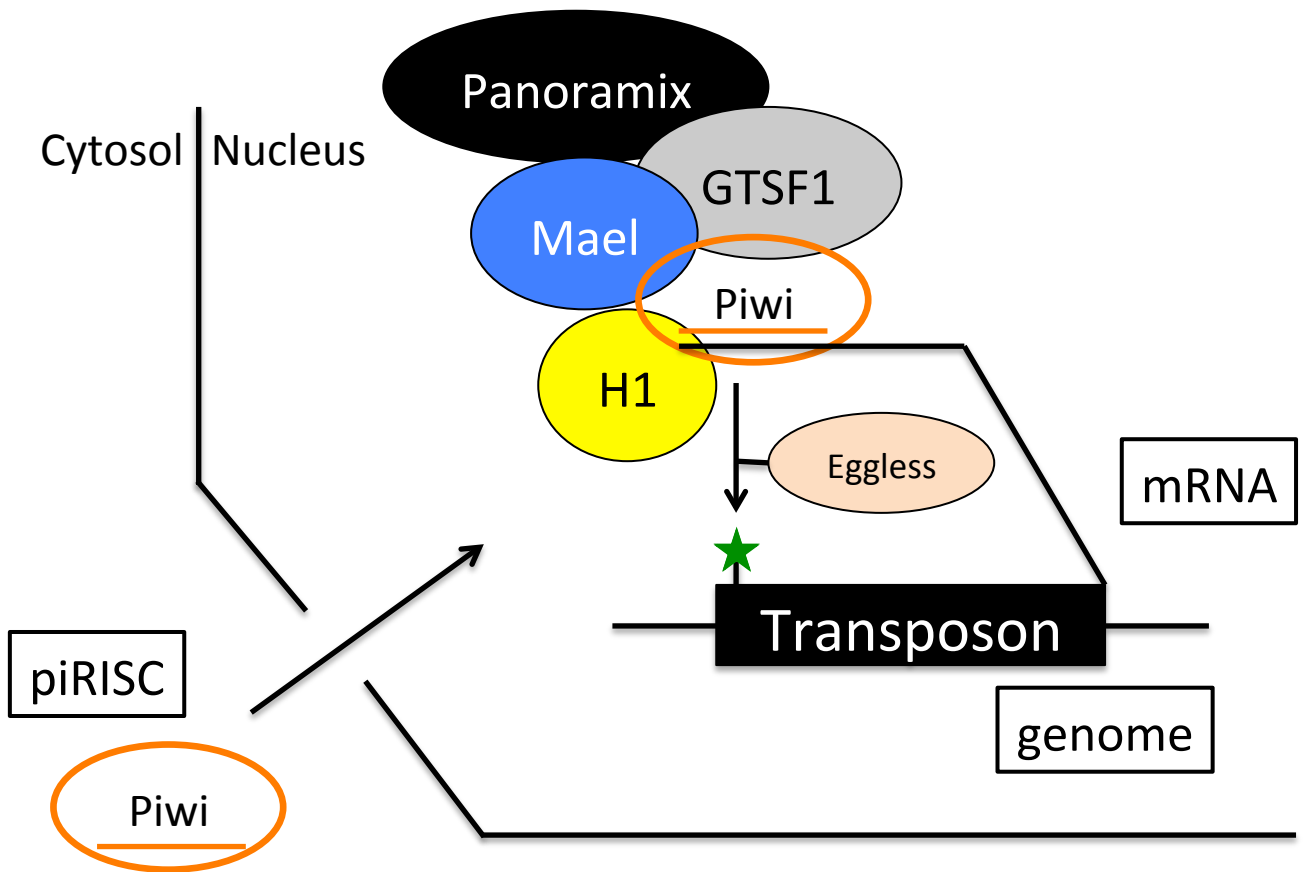


Figure 5. Piwi transposon silencing system in nucleus

After piRISC is imported into nucleus, various factors interacting with Piwi are come and bound. The complex whose center is Piwi acts to genome region of transposon and inserts H3K9me3 showing the green star here, which induces heterochromatinization of this region.

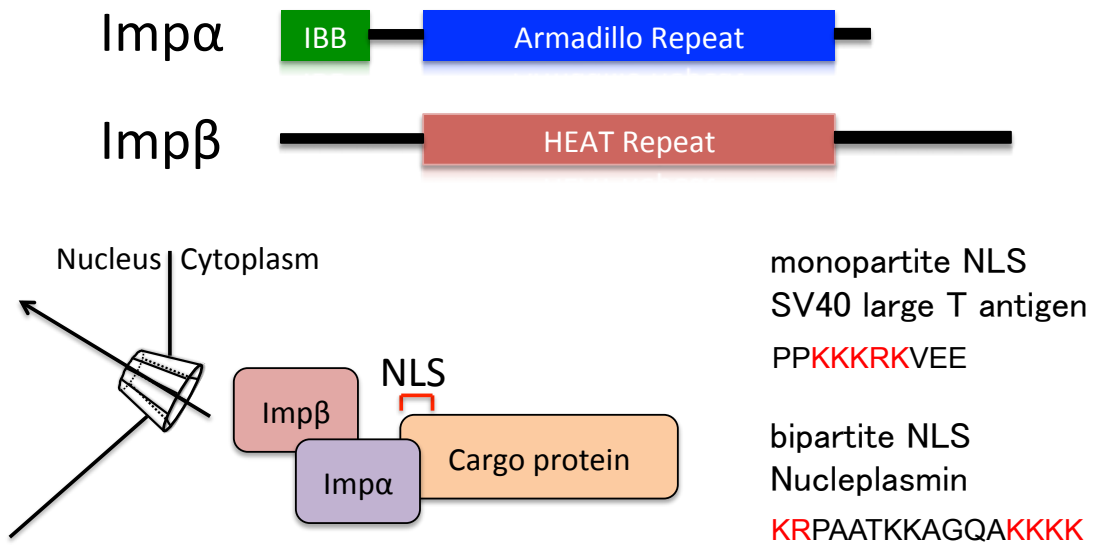


Figure 6. Protein nuclear import system operated by Importin α /Importin β

Imp α has two domains, Imp β binding domain (IBB) and Armadillo repeat (Arm). Imp α binds with Imp β through IBB and with proteins through Arm. Imp β -Imp α -protein trimeric complex goes to nucleus. Representative examples of monopartite NLS and bipartite NLS are SV40-NLS and Nucleoplasmin NLS, respectively. These sequences used in this study are shown here.

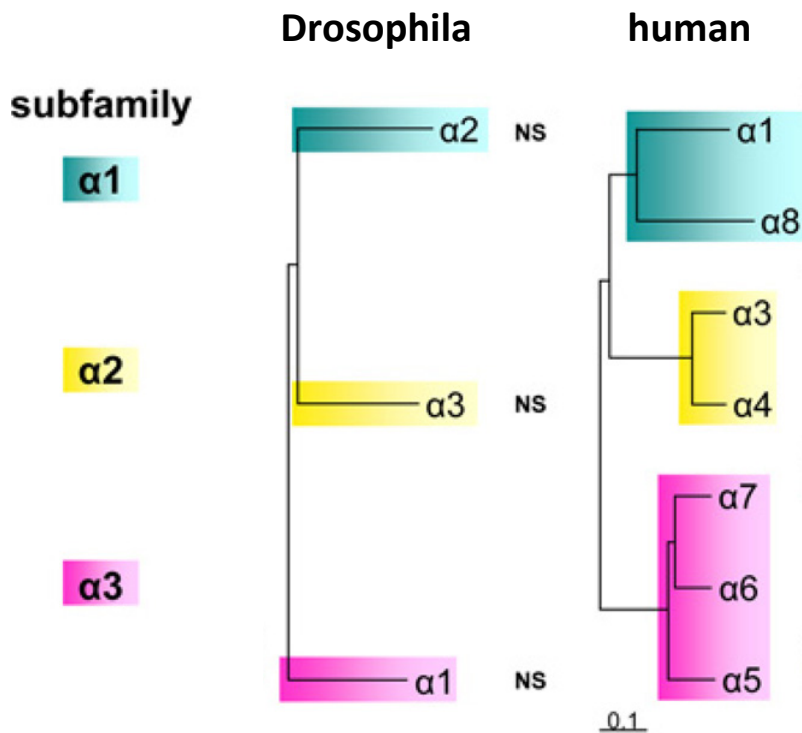


Figure 7. Impα has three clades

Impα has three subfamily, Impα1, Impα2 and Impα3. Drosophila has only one Impα protein in each clades. Here in human for example, human has seven impα genes and Impα1 and Impα8 in Impα1 subfamily, Impα3 and Impα4 in Impα2 subfamily and Impα5, Impα6 and Impα7 in Impα3 subfamily, respectively. This figure was modified from Pumroy and Cingolani, 2015.

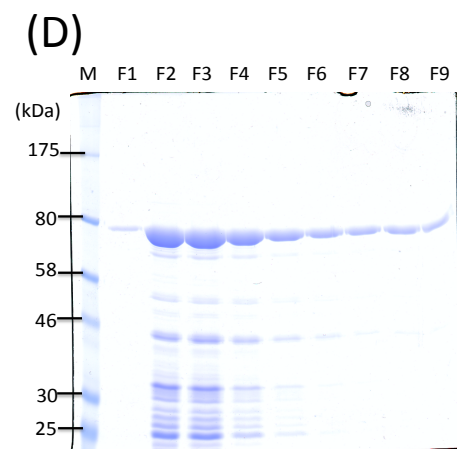
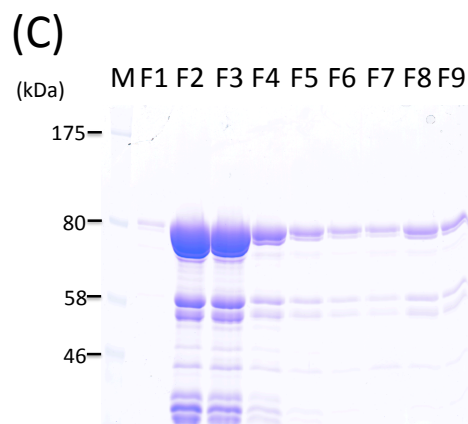
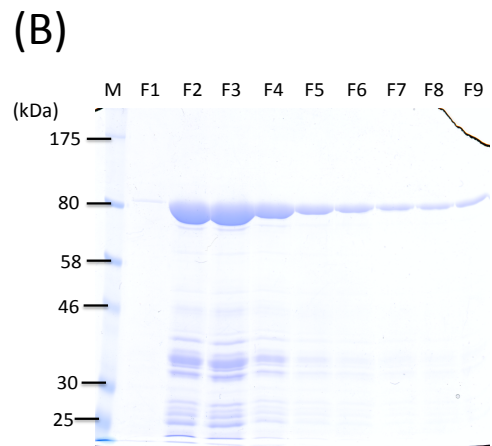
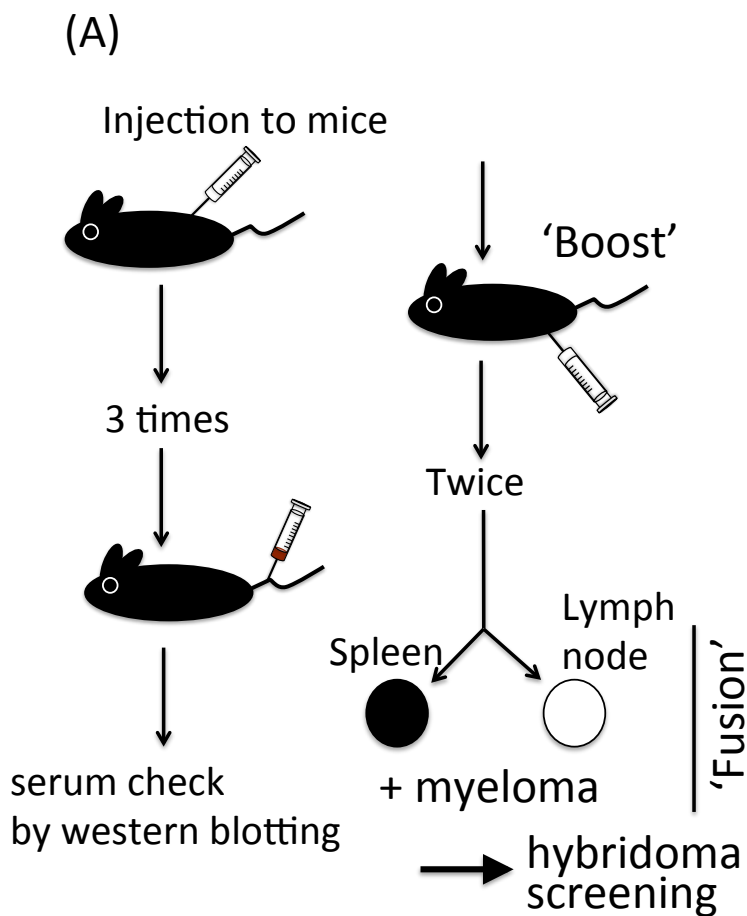


Figure 8. Scheme for antibody production and preparation of GST-Imp α proteins

(A) Scheme for each anti-Imp α antibody production. GST-Imp α 1 (B), GST-Imp α 2 (C) and GST-Imp α 3 (D) were purified from *E.coli*. F2 through F4 was collected and dialyzed. M: Marker, F: Fraction.

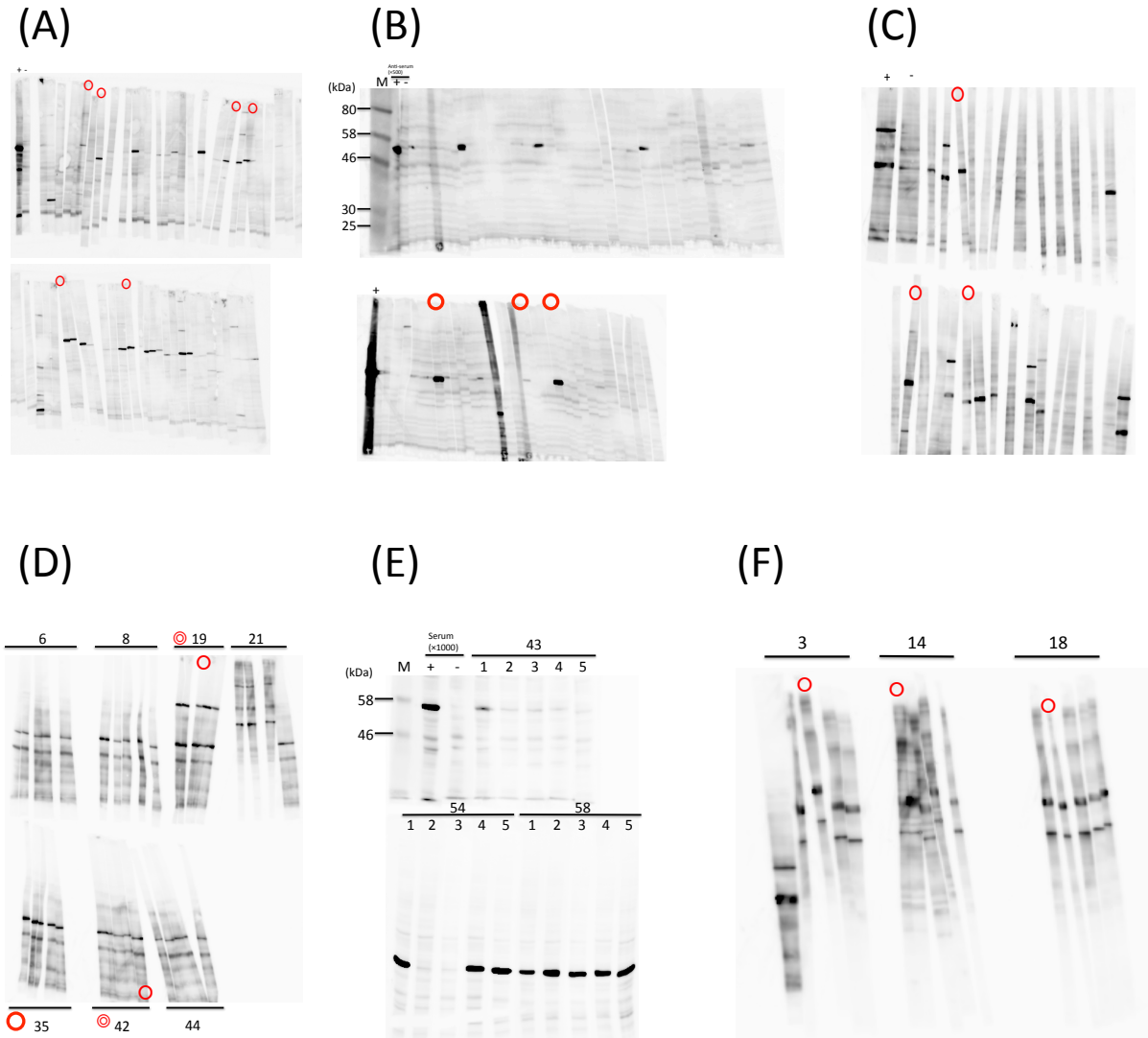


Figure 9. The western blotting screening for each Impα antibody

(A) for Impα1, (B) for Impα2 and (C) for Impα3 were performed for first WB screening after ELISA. (D) for Impα1, (E) for Impα2 and (F) for Impα3 were performed for second WB screening after first screening. “+” shows anti-serum as positive controls and “-” shows only PBS as negative controls. Results shown with red circles are selected and checked for proceeding next step.

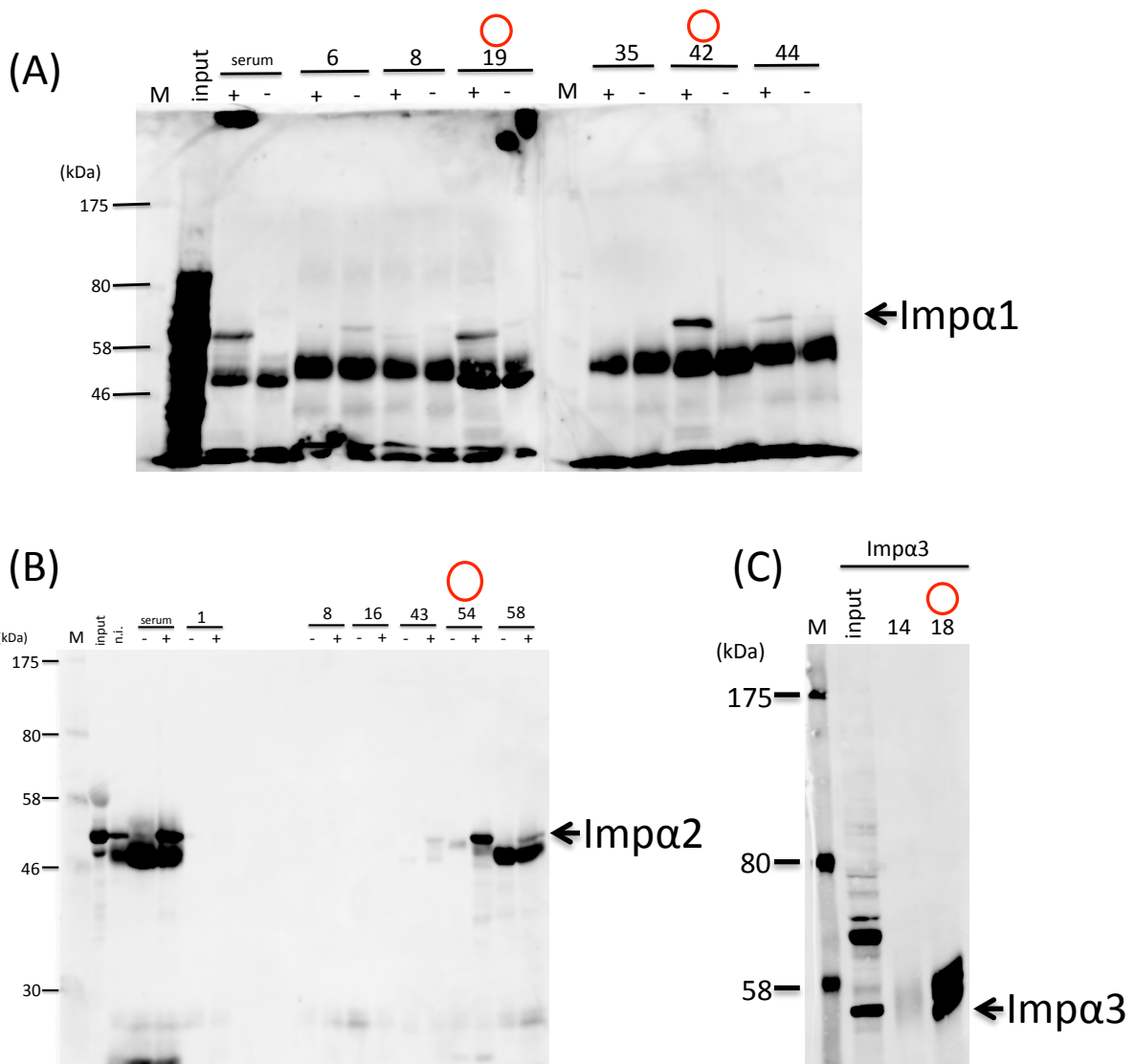


Figure 10. Produced each anti-*Impα* antibody is applied for immunoprecipitation

Western blotting was performed after immunoprecipitating using produced each anti-*Impα* antibody. *Impα1* for (A), *Impα2* for (B) and *Impα3* for (C) were shown and every red circles was proceeded to large-scale culture to make the storages. Although *Impα1* has two circles, 19 was decided to use for experiment.

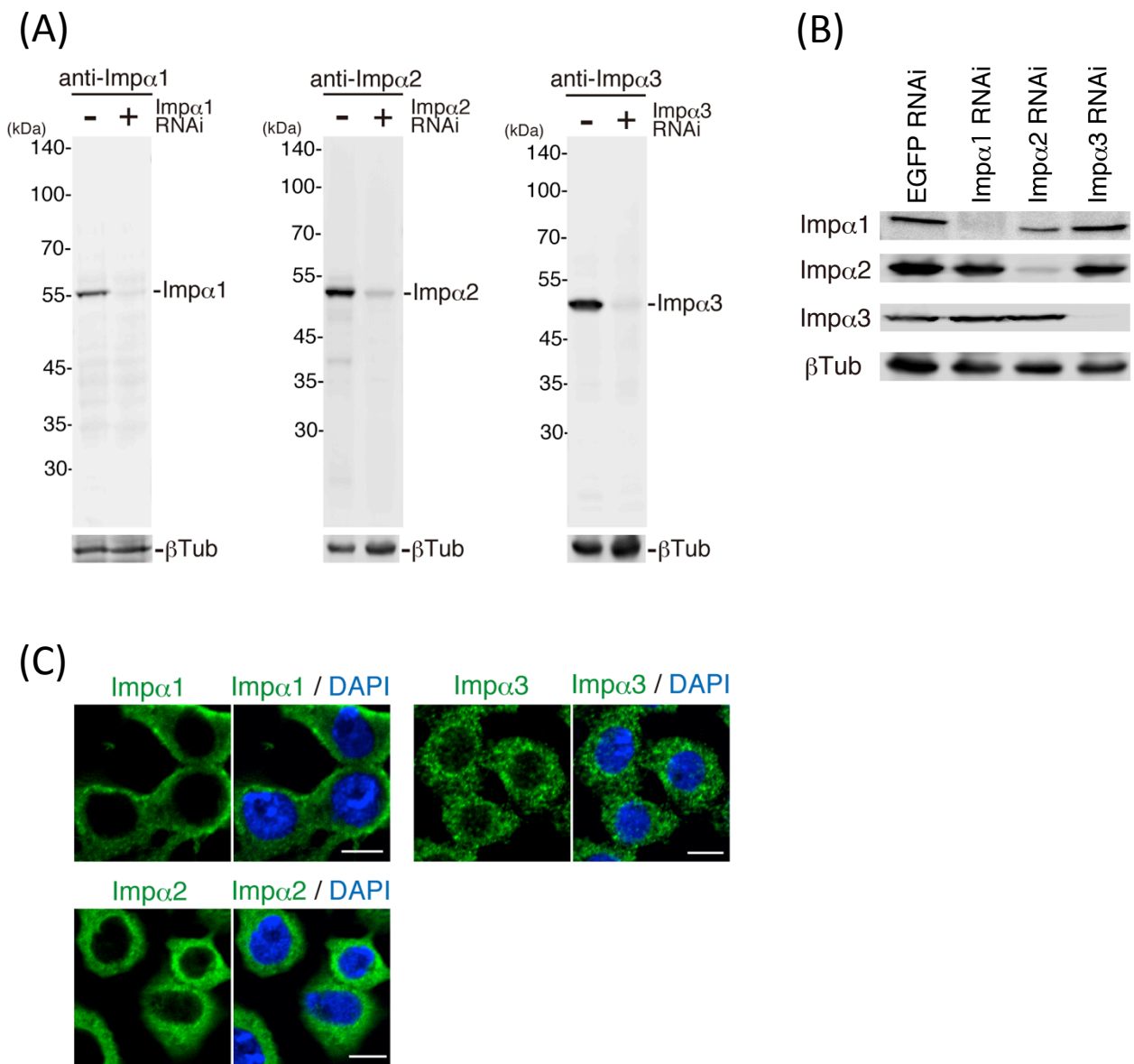


Figure 11. Completed each anti-Imp α antibody is applied for western analysis and immunofluorescence with the effect of knockdown

(A) Western blotting was performed with or without Imp α depletion. (B) Each siRNA was effectively knock-downed with a quite low off-target and every kinds of Imp α antibodies were correct reactivity without cross reaction. (C) Completely produced antibody was also applied for immunofluorescence. Scale bar=5 μ m.

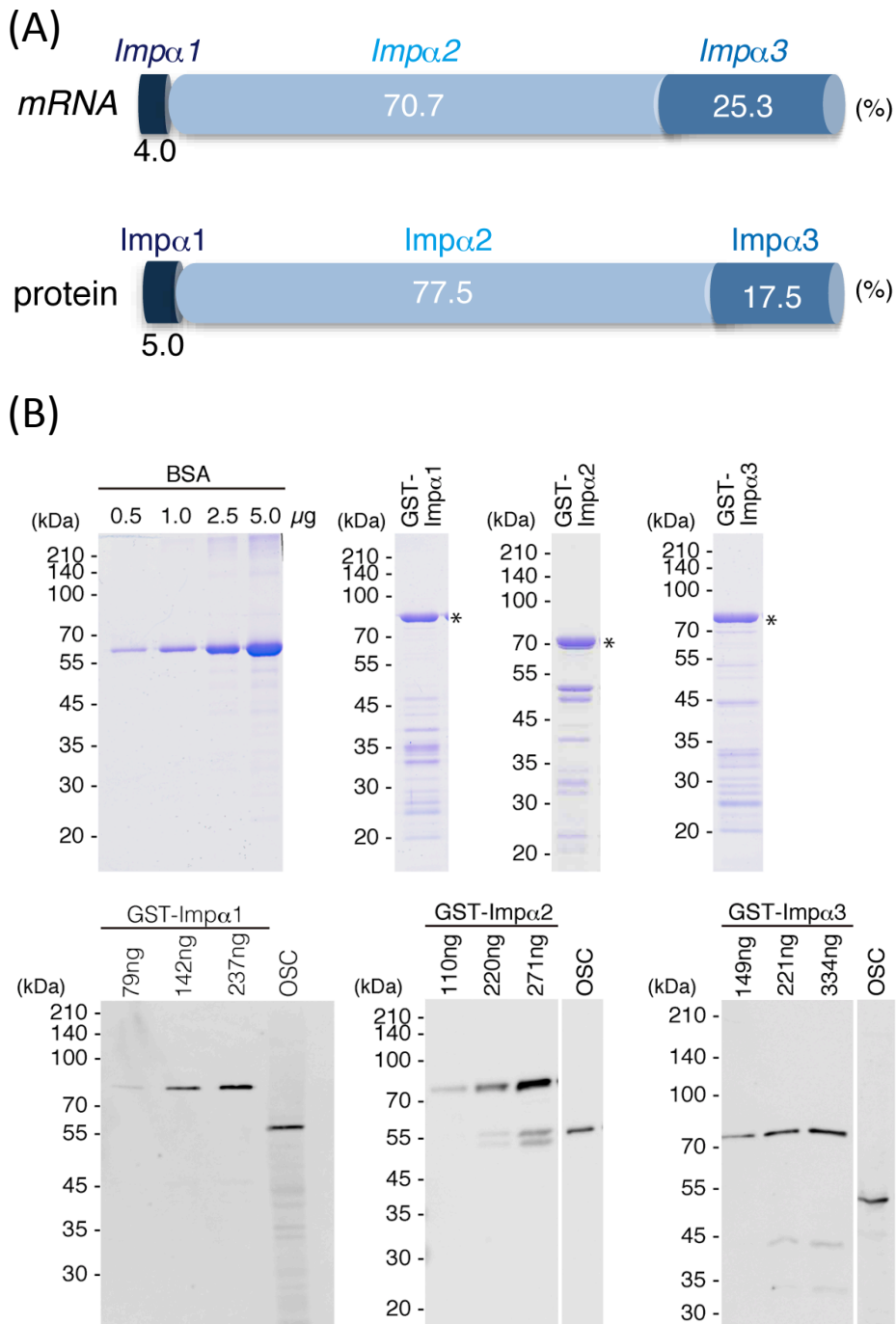


Figure 12. Calculation of the each $Imp\alpha$ ratio in OSC

(A) Top: Previously reported mRNA-seq data is shown the mRNA ratio of each $Imp\alpha$ in OSC (Sumuyoshi *et al*, 2016). Bottom: For the calculation of each $Imp\alpha$ protein level in OSC from the result shown (B). (B) Top: To know the correct amount of each $Imp\alpha$ without degradation products, SDS-PAGE-CBB staining was performed using each purified protein. Bottom: To know how many each $Imp\alpha$ in the 10 μ L OSC lysates and to estimate the ratio of $Imp\alpha$ using standard curve.

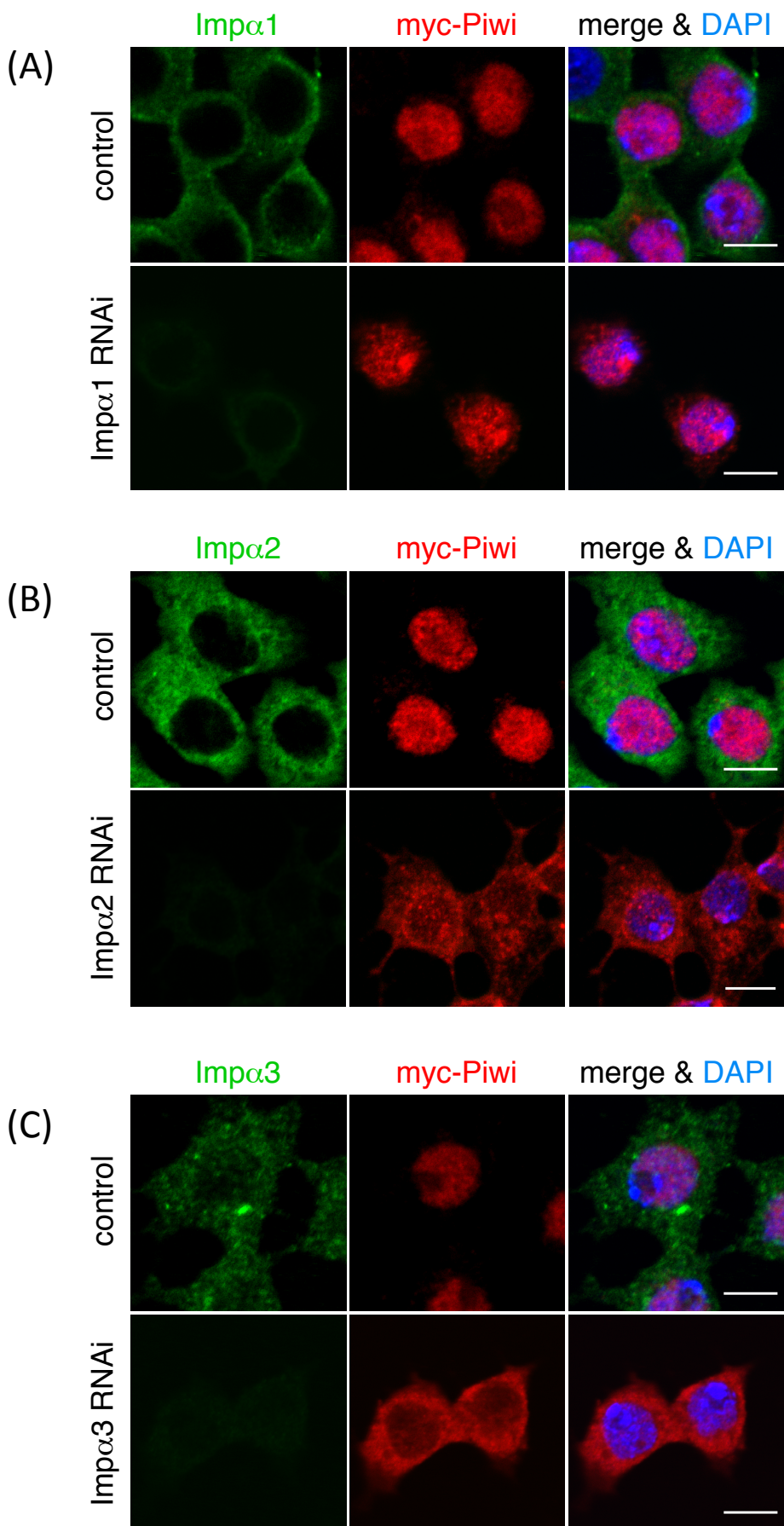


Figure 13. Piwi localization in the *Impα*-depleted condition

The localization of transfected myc-Piwi was not affected by *Impα1* depletion (A). However, when *Impα2* (B) or *Impα3* (C) depleted in OSC, myc-Piwi could not localize to nucleus. DAPI was shown in blue, *Impα* was shown in green and myc-Piwi was shown in red. Scale bar=5μm.

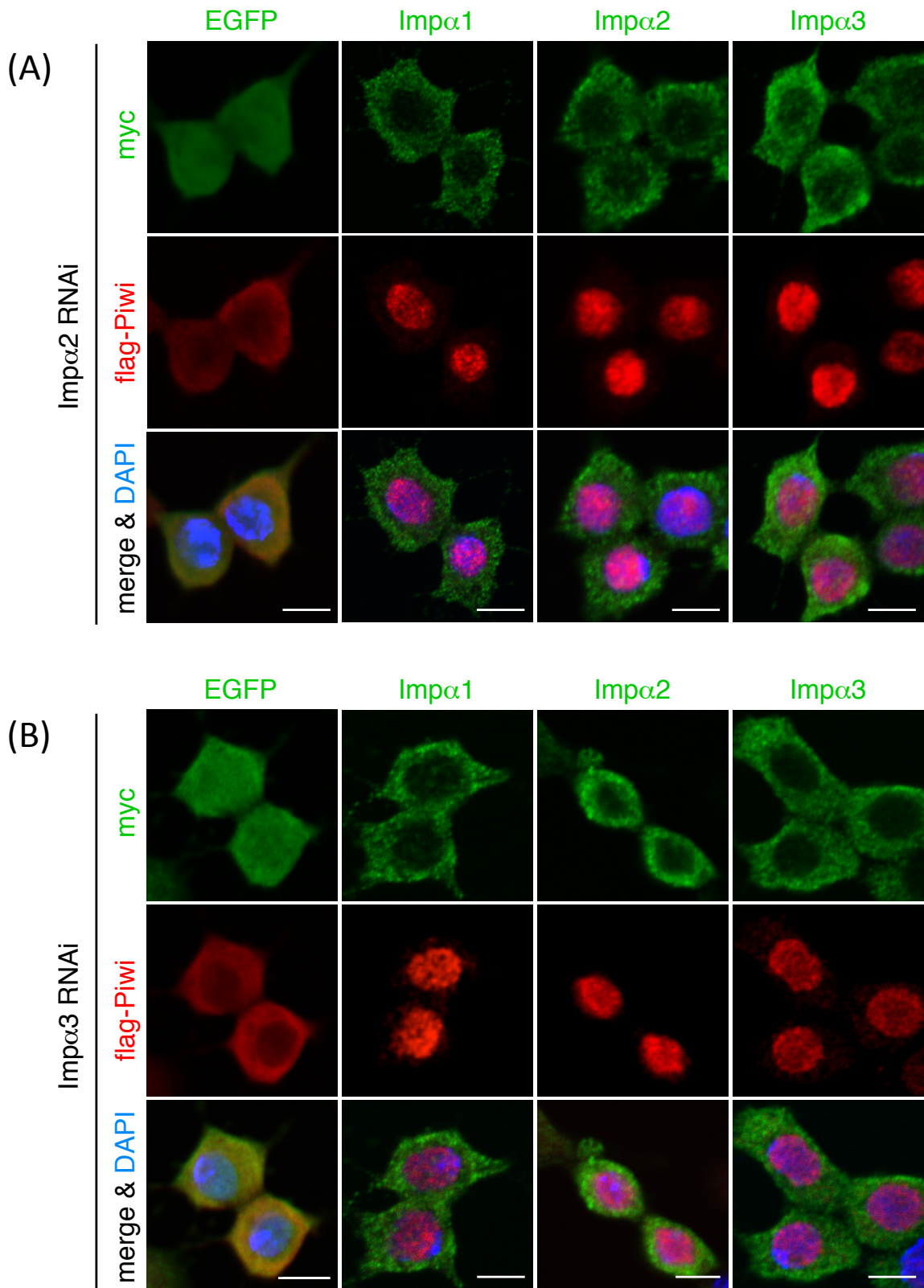


Figure 14. Mislocalized Piwi was rescued by overexpressed Imp α to localize to the nucleus
 In the Imp α 2 or Imp α 3 depleted condition, Piwi shows the abnormal localization. However, each Imp α overexpressed individually in Imp α 2- or Imp α 3- depleted OSC leads to normal Piwi localization. The case of Imp α 2 is shown in (A) and that of Imp α 3 is shown in (B). DAPI was shown in blue, Imp α was shown in green and flag-Piwi was shown in red. Myc-EGFP is used as a negative control. Scale bar=5 μ m.

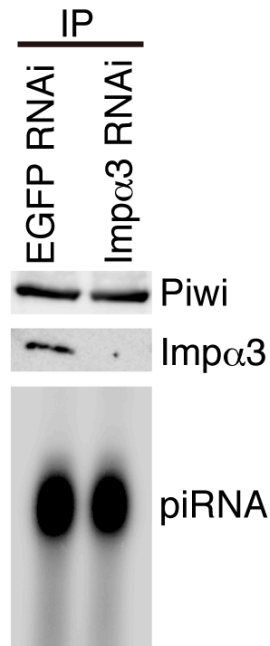


Figure 15. Imp α RNAi does not influence piRNA loading

piRNA loading was not influenced by Imp α 3 RNAi. siEGFP was used as a control. Because Imp α 2 depletion shows heavy cell death, I couldn't harvest the cells enough to perform the immunoprecipitation experiment.

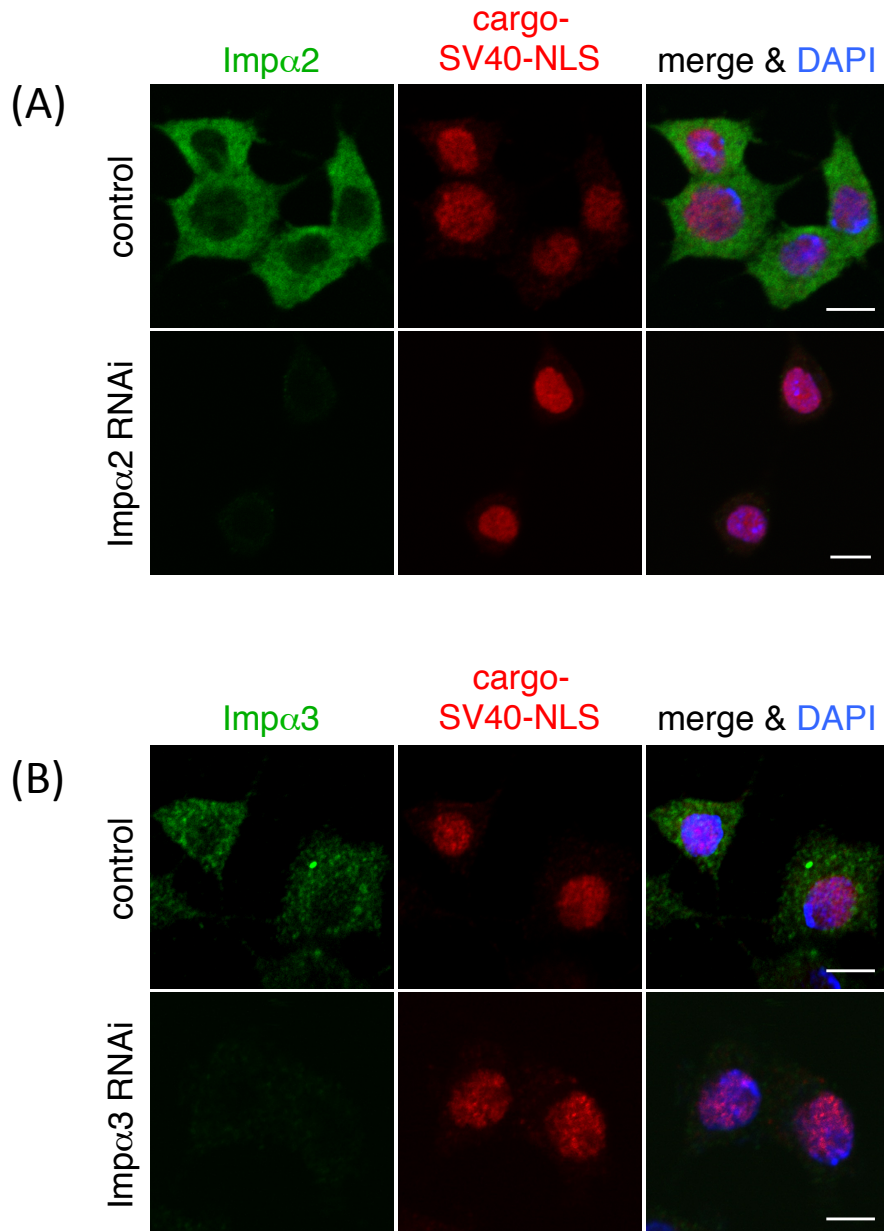


Figure 16. Maelstrom-SV40-NLS was not affected by Imp α 2 or Imp α 3 depletion

In the Imp α 2 or Imp α 3 depleted condition, Piwi shows the abnormal localization. However, the protein combined SV40-NLS was not affected in such condition. The case of Imp α 2 depletion is shown in (A) and that of Imp α 3 is shown in (B). DAPI was shown in blue, Imp α was shown in green and myc-Maelstrom-SV40-NLS (shown as cargo-SV40-NLS) was shown in red. Scale bar=5 μ m.

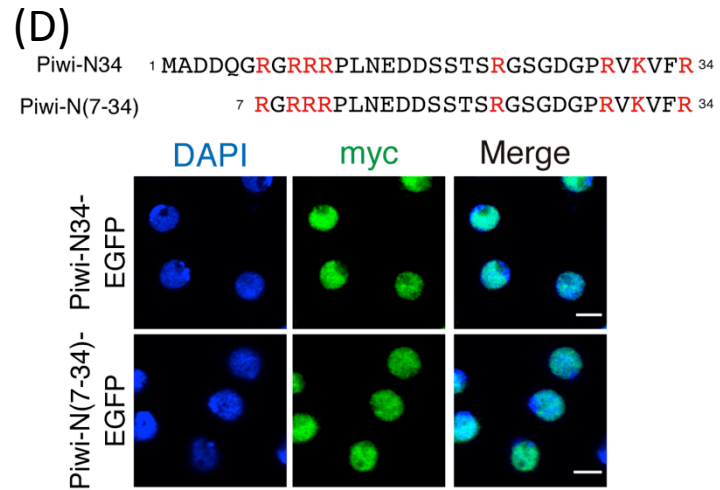
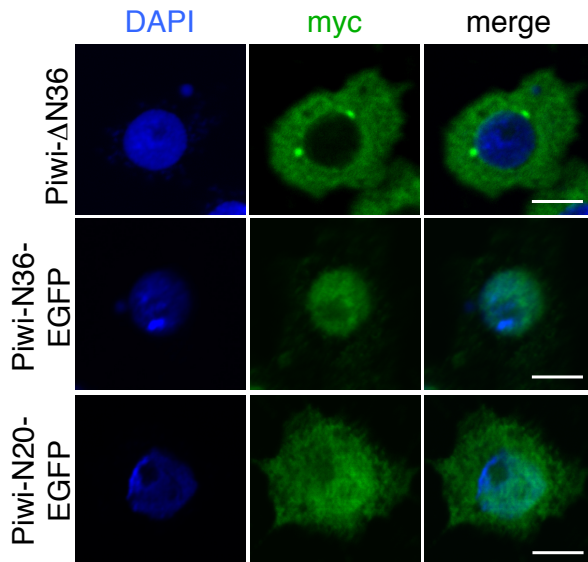
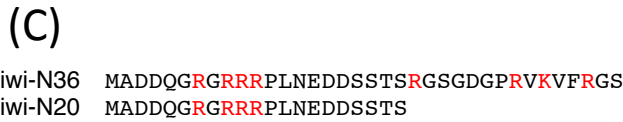
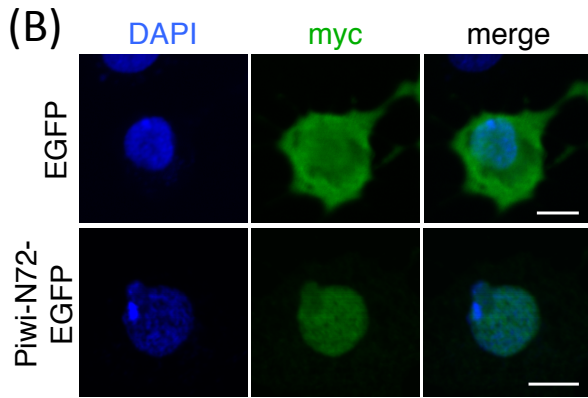
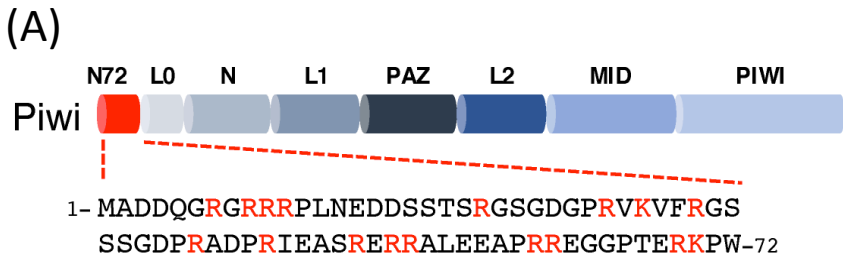


Figure 17. Identification of Piwi-NLS

(A) Piwi-NLS have been regarded as 72 amino acids of Piwi N-terminus (Saito *et al*, 2009). (B) EGFP connected Piwi-N72 to its N-terminus was shown nuclear localization. Scale bar=2μm. (C) Top: Piwi which is deleted 36 amino acids of N-terminus mostly localized to the cytosol. Middle: EGFP connected Piwi-N36 to its N-terminus was shown the nuclear localization. Bottom: EGFP connected Piwi-N20 to its N-terminus spread to throughout the cell. Scale bar=2μm. (D) EGFP connected Piwi-N34 or Piwi-N(7-34) to its N-terminus was shown the nuclear localization. Scale bar=5μm. DAPI was shown in blue and myc was shown in green in all figures here.

(A) Piwi-NLS-M1 MADDQGRGAAALNEDDSSTSRGSGDGP~~RVKVF~~RGS
 Piwi-NLS-M2 MADDQGRGRRRPLNEDDSSTSRGSGDGP~~RVKVF~~RGS
 Piwi-NLS-M3 MADDQGRGRRRPLNEDDSSTSRGSGDGP~~RVKVF~~AGS
 Piwi-NLS-M4 MADDQGRGRRRPLNEDDSSTSRGSGDGP~~RVAVF~~RGS
 Piwi-NLS-M5 MADDQGRGRRRPLNEDDSSTSRGSGDGP~~RVAVF~~AGS

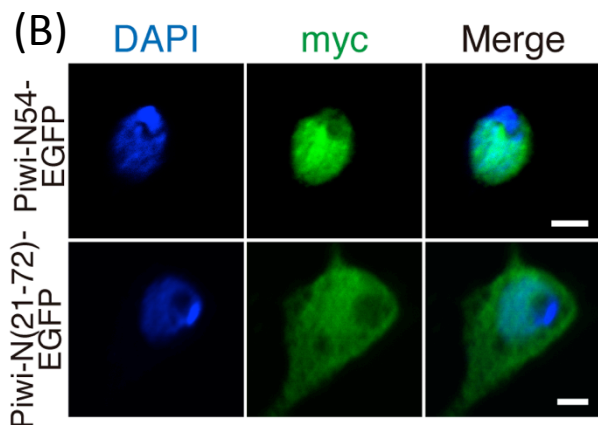
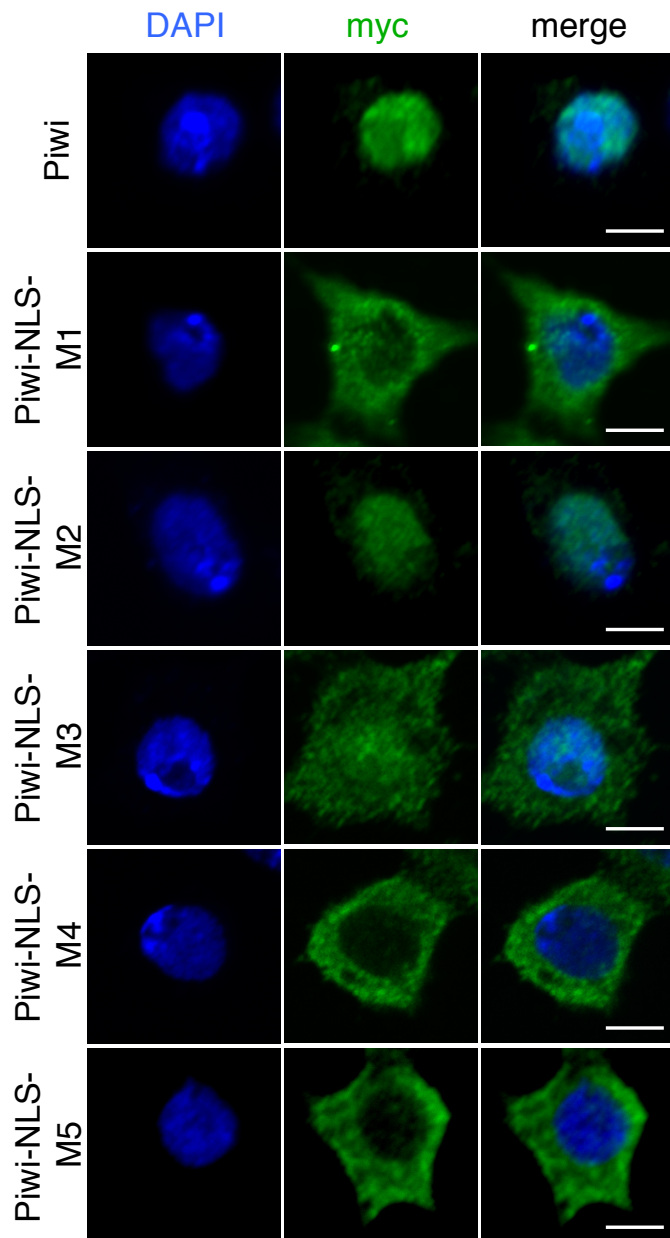


Figure 18. Piwi-NLS is a bipartite NLS
 (A) The subcellular localization of Piwi mutants named Piwi-NLS-M1 through Piwi-NLS-M5 is shown. (B) Top: Piwi-N54-EGFP is localized to the nucleus. Bottom: Piwi-N(21-72)-EGFP can not completely localize to nucleus and protein is spread throughout the cell. DAPI was shown in blue and myc was shown in green. All scale bars in this figure=2µm.

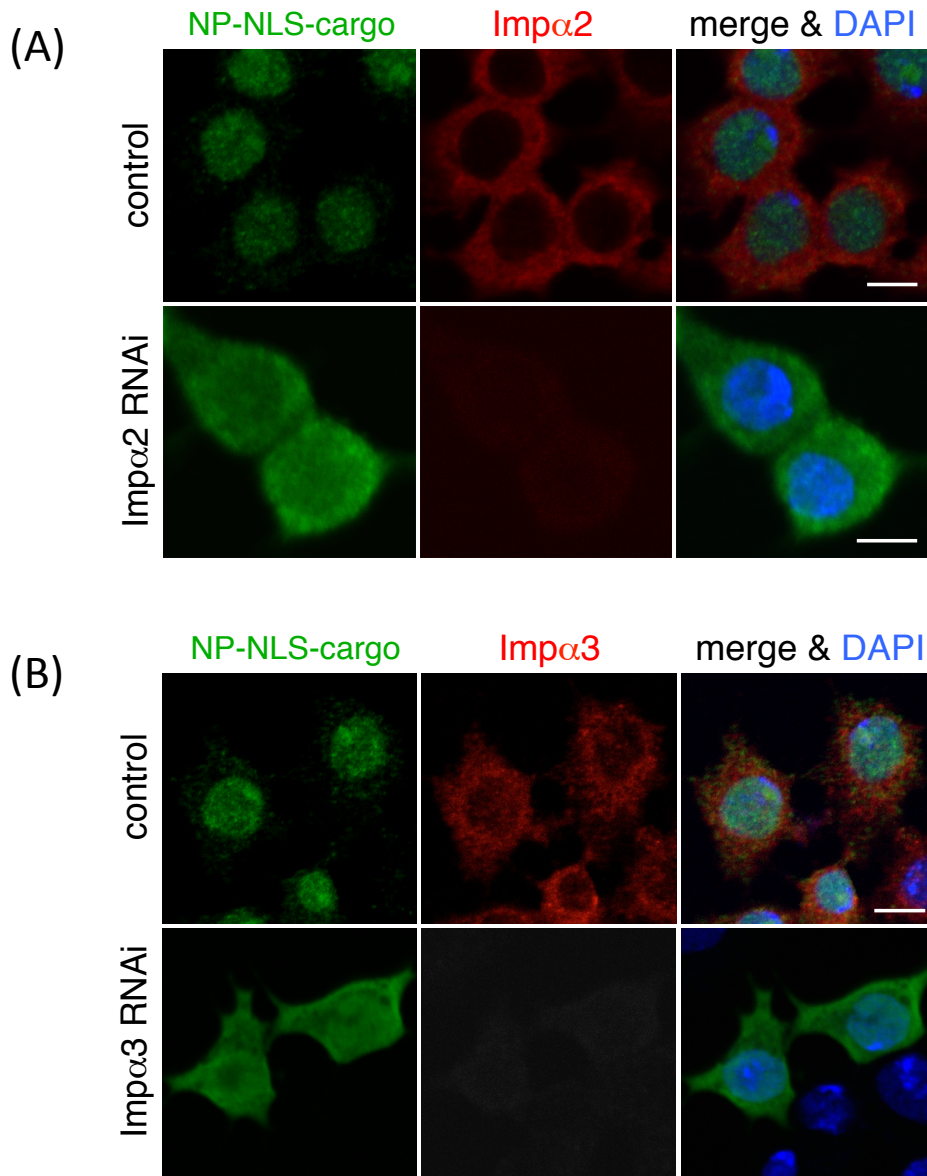


Figure 19. NP-NLS-EGFP was affected by Imp α 2 or Imp α 3 depletion

Piwi has a bipartite NLS. The representative example of a bipartite NPS Nucleoplasmin NLS (NP-NLS) was connected to EGFP. In the Imp α 2 or Imp α 3 depleted condition, the subcellular localization of this mutant was wrong. The case of Imp α 2 depletion is shown in (A) and that of Imp α 3 is shown in (B). DAPI was shown in blue, Imp α was shown in red and myc-NP-NLS-EGFP (shown as NP-NLS-cargo) was shown in green. Scale bar=5 μ m.

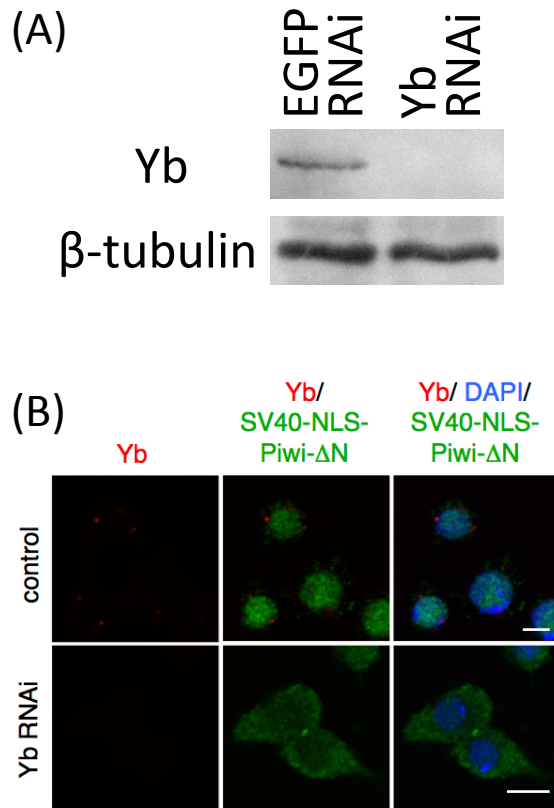


Figure 20. The localization of SV40-NLS-Piwi Δ N is piRNA-dependent.

(A) Yb, one of the most important factors of piRNA biogenesis, was correctly knock-downed by siRNA. siEGFP was used as a negative control for siYb. (B) Piwi of lacking 36 amino acids of N-terminus connected with SV40-NLS, which is meant Piwi-NLS is replaced by SV40-NLS, is shown a piRNA-dependent subcellular localization. DAPI was shown in blue, Yb was shown in red and myc-SV40-NLS-Piwi Δ N was shown in green. Scale bar=5 μ m.

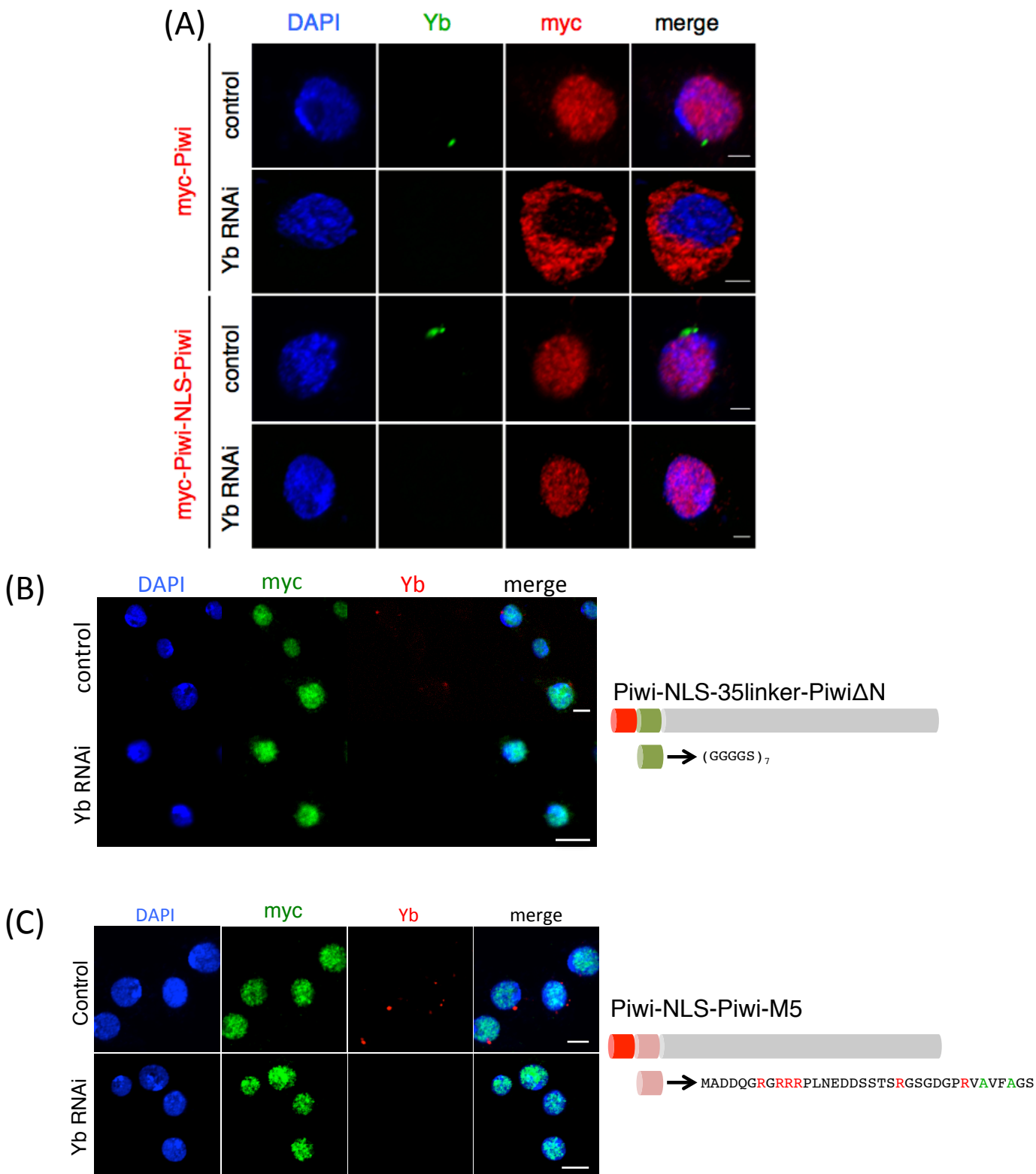


Figure 21. Elongated Piwi-NLS led Piwi to nucleus piRNA-independently

(A) Piwi-NLS-Piwi, which elongated Piwi-NLS to Piwi wild type, is shown the piRNA-independent subcellular localization. DAPI was shown in blue, Yb was shown in green and myc-Piwi-NLS-Piwi was shown in red. Scale bar=2 μ m. (B) Piwi-NLS-35linker-Piwi Δ N is also shown localizing piRNA-independently. The 35linker inserted is seven GGGGS repeats. DAPI was shown in blue, Yb was shown in red and myc-Piwi-NLS-35linker-Piwi Δ N was shown in green. Scale bar=5 μ m. (C) Piwi-NLS-Piwi-NLS-M5 is also shown the nuclear localization although Piwi-M5 is completely localizing to cytoplasm (Fig.10). DAPI was shown in blue, Yb was shown in red and myc-Piwi-NLS-Piwi-NLS-M5 was shown in green. Scale bar=5 μ m.

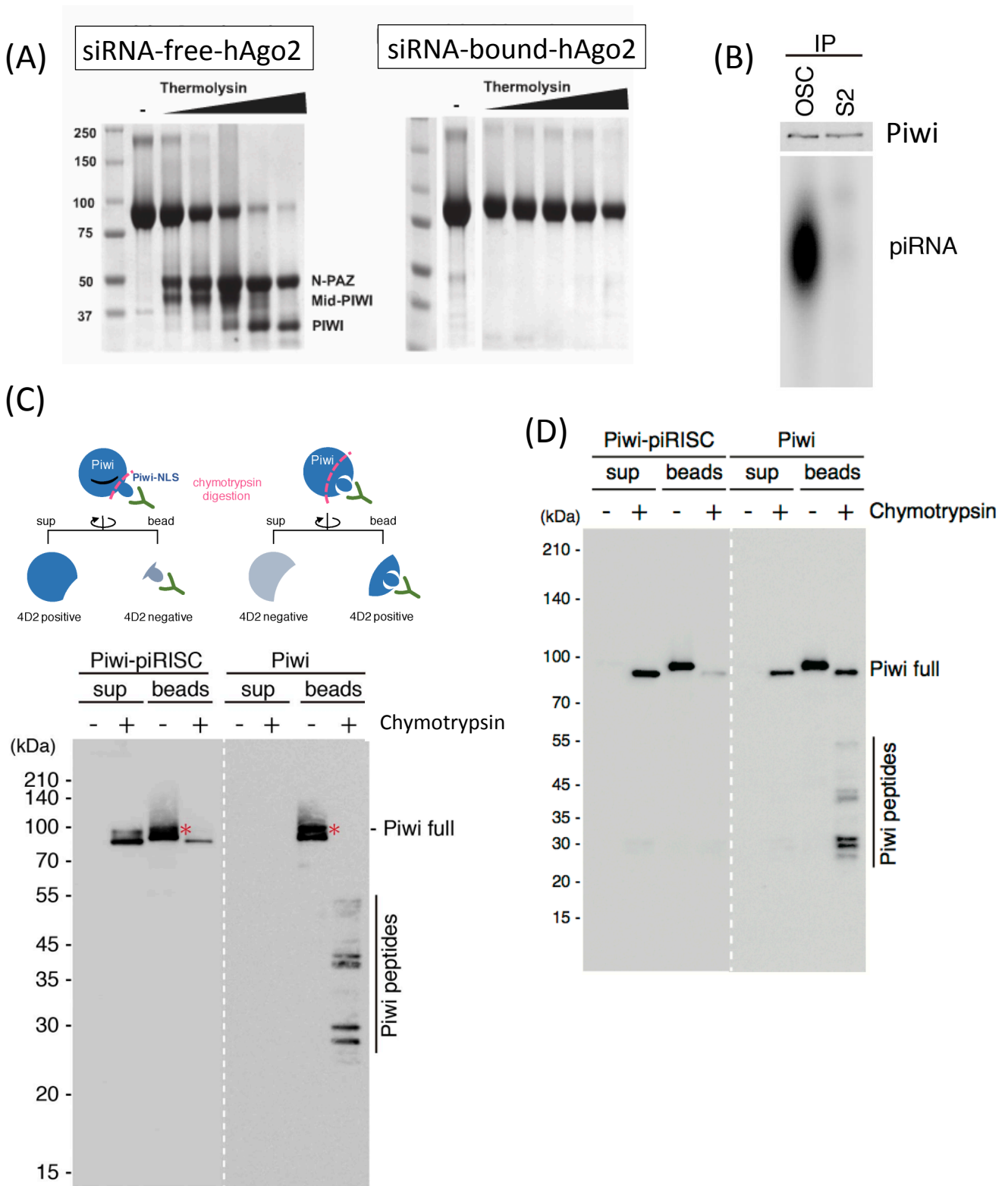


Figure 22. Limited proteolysis assay reveals Piwi that does not load piRNA is more instability than piRISC and Piwi protects its N-terminus until piRNA loading

(A) Human Ago2 will get stability when siRNA is loaded (modified from Elkayam *et al.*, 2012). (B) Overexpressed Piwi in S2 cells do not form piRISC. (C) Limited proteolysis assay indicates structural change between piRISC and piRNA-free Piwi unveiled by western blotting using anti-Piwi 4D2 antibody. (D) Same assay as (C) using OSC cells. Piwi that does not form piRISC is from the depletion of GasZ, which might be considered as an essential factor of piRNA biogenesis that is located on mitochondrion.

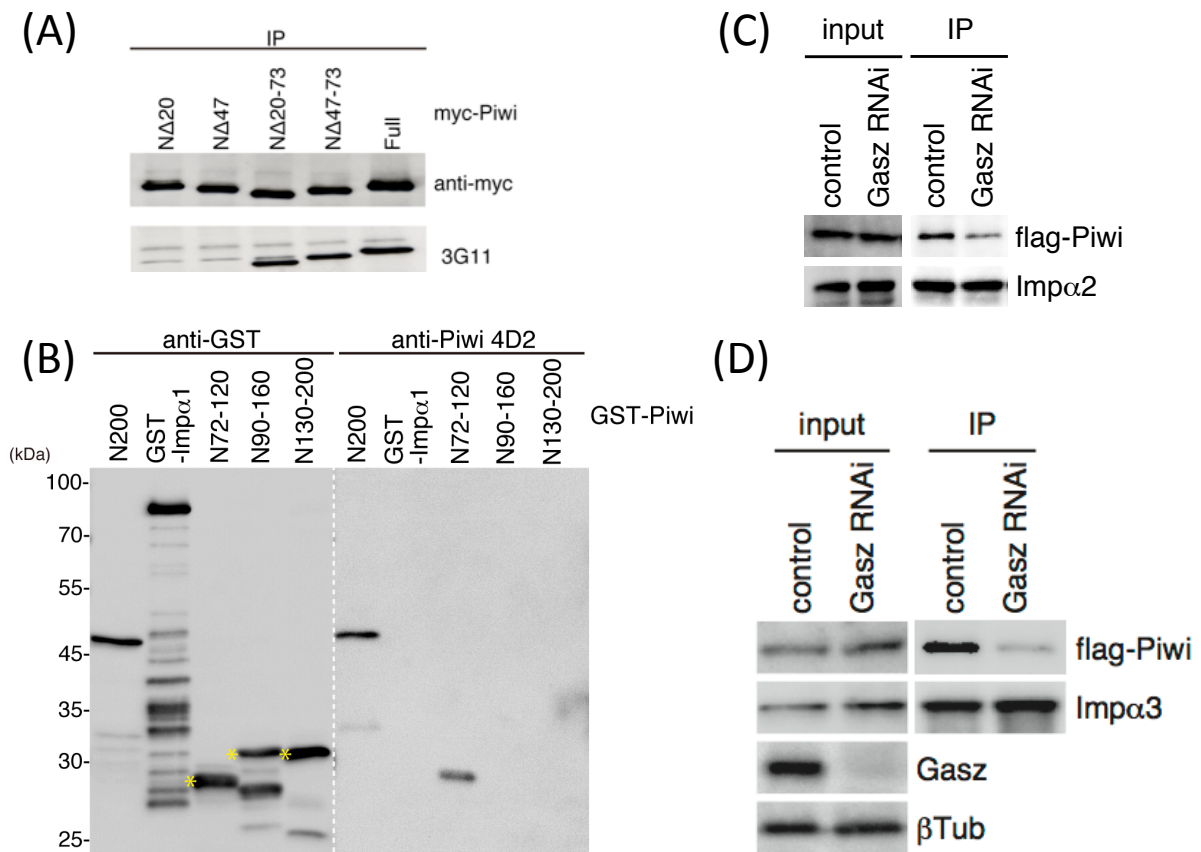


Figure 23. Piwi-Imp α binding activity of piRISC is stronger than piRNA-free state

(A) The epitope of anti-Piwi monoclonal antibody 3G11 is PiwiN1-20. (B) The epitope of anti-Piwi monoclonal antibody 4D2 is PiwiN72-90. Yellow asterisks shows the proteins indicated.

(C) and (D) Piwi-Imp α 2 (C) or -Imp α 3 (D) binding assay was performed by immunoprecipitation and its binding was detected by western blotting.

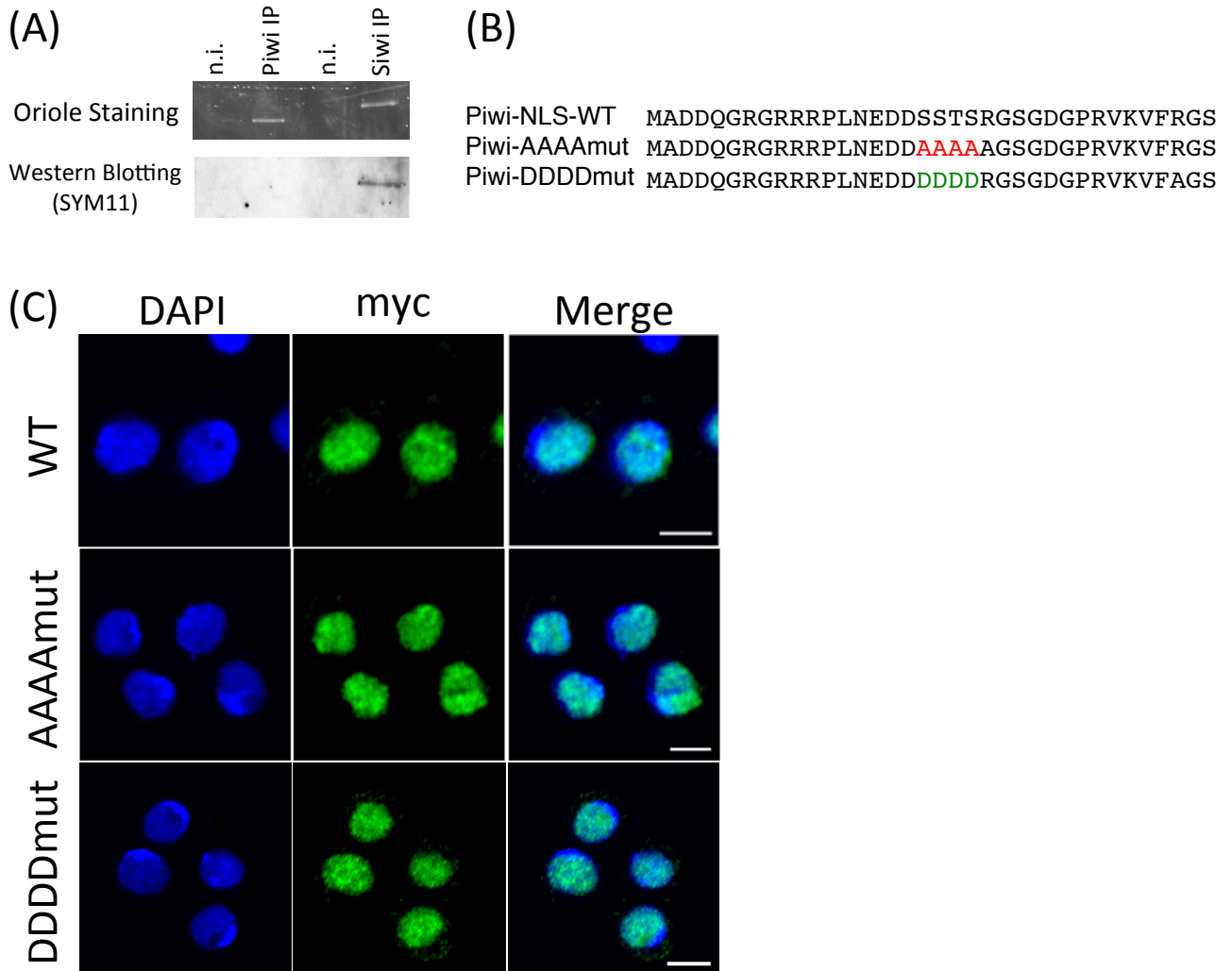


Figure 24. sDMA and phosphorylated modifications in Piwi-NLS are not involved in Piwi nuclear localization

- (A) *Drosophila* Piwi IP or *Bombyx mori* Siwi IP show that only Siwi has sDMA modification by SYM11 anti-sDMA antibody.
- (B) The sequences show how mutated to make the state of constitutive non-phosphorylation (AAA shown in red) and phosphorylation (DDDD shown in green).
- (C) Immunofluorescence indicates the phosphorylation of Piwi-NLS is not involved in Piwi nuclear localization.

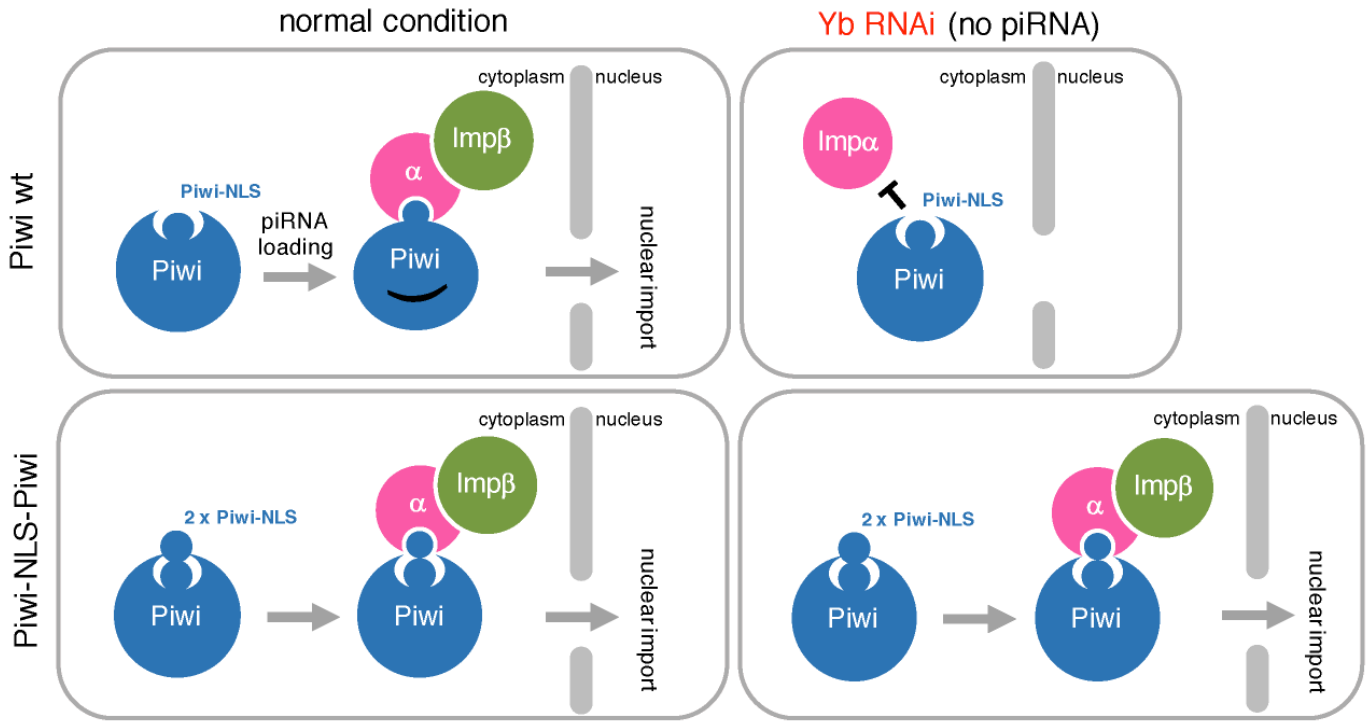


Figure 25. Regulatory mechanism of Piwi nuclear import

When Piwi does not form piRISC, Piwi-NLS is hidden by Piwi itself structurally. Once Piwi loads piRNA, Piwi-NLS appears and is recognized by Imp α . Then Piwi transports into the nucleus. If Piwi-NLS appears in a piRNA-free condition, for example Piwi-NLS is added to Piwi full length or linker sequences are inserted between Piwi-NLS and rest of Piwi in the Yb-depleted condition, such Piwi mutants can localize to the nucleus apart from its function. Although such conditions may not occur in nature, the importance of Piwi N-terminus about Piwi nuclear localization was shown by this paper using *in vitro* or *in vivo* biochemical experiments.

Piwi 1- MADDQGRGRRRPLNEDD--SSTSRGSGDGPRVKVFRGS -36
MIWI2 1- MS-GRARVRARGITTGHSAREVGRSSRDLMVTSASPG- -36

Figure 26. Alignment of Piwi-N36 sequence and MIWI2-N36 sequence

N-terminal 36 amino acids sequences of Piwi of *Drosophila* and MIWI2 of mouse are aligned. The letters shown in red mean basic acids, which are said that they are quite important amino acids for recognition by Imp α .

Tables

Table 1. Sequences of PCR primers used in this study.

Plasmid Construction	Primer Name	Sequence	Primer Name	Sequence	
AcM-PiwiN20-EGFP	PN20E-F	GAATTCGACAGATATATGGTGAGCAAGG	PN20E-R	AGTAGAGGAATCATCTTCGTTAAGTGA	
	AcM-PiwiN36-EGFP	PN36E-F	GAATTCGACAGATATATGGTGAGCAAGG	PN36E-R	AGATCCCTCTGAATACTTTCACCCCG
		PN-M1-F	GCCGCCCTTAACGAAGATGATTCCTCTACTTCCC	PN-M1-R	GGCGGCTCCACAGTCCCTGATCATCAG
	AcM-Piwi-NLS-M1	PN-M2-F	GCAGGTAGTGGTGTGGGGCCG	PN-M2-R	GGAAAGTAGAGGAATCATCTTCGT
		PN-M3-F	GCAGGATCTTCATCAGGTGACC	PN-M3-R	GAATACTTTCACCGCGCGCC
	AcM-Piwi-NLS-M2	PN-M4-F	GCAGTATTCAGAGGATCTTCATCAGGT	PN-M4-R	CACCCGGGCCCCATCCAC
		PN-M5-F	GCAGTATTCGAGGATCTTCATCAG	PN-M5-R	CACCCGGGCCCCATCCAC
	AcM-ΔPiwiN36-Piwi	PNΔ36-F	TCATCAGGTGACCCGAGAGC	PNΔ36-R	AAGCTTATATCTGCAGAATTCGGGTACC
		Mael-SN-F	CTTCTTTTTGGAGGTTTTTAAGTTTTCCCAT	Mael-SN-R	AGAAAGGTAGAAAGAAATAACTCGAGTCTAGAGG
	AcM-Mael-SV40-NLS	Imp α1-F	GCAGAAAACGAAACAGCTTGAG	Imp α1-R	CCGCTAAATAGCATTGGAATCATTTTC
		Imp α2-F	ACATGAAAACGAGGAGGCTTACAAG	Imp α2-R	TGTTGAAAGAGTTCCAGACTTGTCTA
	AcM-impα2-sir	Imp α3-F	CCGATGCAACCAAGCCCG	Imp α3-R	CCGCCGCCCTTTGCCAG
		PNΔ20-73-F	GGTGACCAATATGATTACCTGGATAC	PNΔ20-73-R	AGTAGAGGAATCATCTTCGTTAAGTG
AcM-PiwiΔN47-73	PNΔ47-73-F	GGTGACCAATATGATTACCTGGATAC	PNΔ47-73-R	TATACGAGGATCCGCTCTCCG	
	AcP-F	GCTGATGATCAGGACGTGGA	AcP-R	TCCATGGTGGCTAGGCCGAT	
pGEX-impα1	Gimpa1-F	AGAGGAATTCATGCTGCCAGCCACAACAG	Gimpa1-R	AGAGCTCGAGCTAAAAGTTAAATCCCGTGTGG	
	Gimpa2-F	AGAGGAATTCATGATGTAAGCCGATCTAACTCAC	Gimpa2-R	AGAGCGCGGTTAGAACGTTAGCCACCTT	
pGEX-impα3	Gimpa3-F	AGAGGAATTCATGACGCTATGGAGCAAAATCG	Gimpa3-R	AGAGCTCGAGTTAAAAGTTAAATGATTCATCGTTAGCC	
	SN-Piwi-F	TCATCAGGTGACCCGAGAGC	SN-Piwi-R	TTATTATACCTTTCTCTCTTTTTGGAGGAA	
AcM-SV40-NLS-Piwi-ΔN	PN34E-F	GAATTCGACAGATATATGGTGAGCAAGG	PN34E-R	TCTGAATCTTTCACCCGCGG	
	PN(7-34)E-F	GGTGAGCCGAGGGCTC	PN(7-34)E-R	CATAAGCTTCTCAGGTTCTTCTCAGA	
AcM-Piwi-N(7-34)-EGFP	PN54E-F	GAATTCGACAGATATATGGTGAGCAAGG	PN54E-R	TCTTCTCTCTTCTGAAAGCCCTCTATAGC	
	PN(21-72)E-F	TCCCGAGGTAGTGGTGTGGTGG	PN(21-72)E-R	AAGCTTGTTCAGGCTCTTCTCAGAGATC	
AcM-NP-NLS-EGFP	NP-sense	AAGCTTAAGCCAGCCGCCACCAAGAGCCGCCAAGAAAGAAATTC	NP-antisense	GAATTCCTTCTTTCTTTCTTTGCTTGGCCGCCCTTCTTGGGGCTGCTCGCTTAAGCTT	
	SV40-sense	AAGCTTCCTCCAAAAAAGAGAAAGGTAGAAAGAAATTC	SV40-antisense	GAATTCCTTCTTCTTCTTTGCTTGGCCGCCCTTCTTGGGGCTGCTCGCTTAAGCTT	
AcM-Piwi-NLS-35linker-PiwiΔN	Link-F	TCAGGTGACCCGAGAGCC	Link-R	TGAAGATCGTCTGAATACTTTCACCCCG	
	Link-sense	* Too long to write here. See Method.	Link-antisense	* Too long to write here. See Method.	
AcF-Piwi	F-Piwi-I-F	CTAGCCACCATGGGAGACTACAAAAGCCATGACCGGTG	F-Piwi-I-R	GGTACCAGCTTGTCTTCTGTCATCGTCATCCTTGTAAATCG	
	F-Piwi-V-F	AACAAGCTTGGTACCAGAAATCTG	F-Piwi-V-R	TCCCATGGTGGCTAGCCCGAT	
AcM-Piwi-NLS-Piwi	PN36-I-F	TGCAGATATAAGCTTGTGATGATCAGGGACGTGG	PN36-I-R	TCCCATGATCAGCACCACTACCTCGGGAAGTAGAG	
	PN36-V-F	GCTGATGATCAGGACGTGGA	PN36-V-R	AAGCTTATATCTGCAGAATTCGGTACC	
AcM-PiwiN72-EGFP	PN72E-I-F	GACCTGAACAAGCTTGTGATGATCAGGGACGTGG	PN72E-I-R	ATATCTGCAAGATTCACCGGCTTTCGCCTCTGG	
	PN72-V-F	GAATTCGACAGATATATGGTGAGCA	PN72-V-R	CATAAGCTTGTTCAGGCTTCTTCTCA	
AcM-Piwi-NΔ20	PNΔ20-I-F	GCTTGTACCAGAAATCTCCAGGATGTTGGTGTGATG	PNΔ20-I-R	GATATCTGCAAGATTTTATAGATAAATAAACTCTTTTTCGAG	
	PNΔ47-V-F	GCTTGTACCAGAAATCTCCAGGATGTTGGTGTGATG	PNΔ47-V-R	GATATCTGCAAGATTTTATAGATAAATAAACTCTTTTTCGAG	
pGEX-Piwi-N72-120	PN72-120-I-F	AGAGGAATTCCTGGGTGACCAATATGATTACCTGG	PN72-120-I-R	TCTCGCGCCGCCCTCCACGCTGATAATGAACGATCCG	
	PN90-160-I-F	AGAGGAATTCGGAAACCCGATGGCCGCTCCCG	PN90-160-I-R	TCTCGCGCCGCCCTCGAAATTCCTCGTGGTGAACAG	
pGEX-Piwi-N130-200	PN-130-200-I-F	AGAGGAATTCCTGATGGAGTTTTGTCCCAATCATGC	PN-130-200-I-R	TCTCGCGCCGCCCTATTAGATTTAAAGACTTGCAAAAAGCCGGG	
	4A-F	GCCGCCGAGGTAGTGGTGA	4A-R	GGCGGCATCATCTTCGTTAAGTGGACG	
AcM-Piwi-AAAmut	4D-F	GACGACCCGAGGTAGTGGTGGGGCC	4D-R	GTCTCATCATCTTCGTTAAGTGGACGCCCT	

Table 2. Sequences of siRNAs used in this study.		
siRNA	<i>*Italic letters show RNA, normal ones show DNA.</i>	
Gene	sense	antisense
EGFP	<i>GGCAAGCUGACCCUGAAGUTT</i>	<i>ACUUCAGGGUCAGCUUGCCTT</i>
Luc	<i>CGUACGCGGAAUACUUCGATT</i>	<i>UCGAAGUAUUCGCGUACGTT</i>
Yb	<i>GGGGUACAUCAACCAAGCUTT</i>	<i>AGCUUGGUUGAUGUACCCCTT</i>
Impα1	<i>AUGCUCUUCAGUGGACGUGTT</i>	<i>CACGUCCACUGAAGAGCAUTT</i>
Impα2	<i>CUCUGCAGCAGCAGGAGAATT</i>	<i>UUCUCGUGCUGCUGCAGAGTT</i>
Impα3	<i>AGGCAGCCGCAGACGCCACTT</i>	<i>GUGGCGUCUGCGGCUGCCUTT</i>
Gasz	<i>CGCUCGAAACCAGCUCCUUTT</i>	<i>AAGGAGCUGGUUUCGAGCGTT</i>

Tables. Primers (Table 1) and siRNAs (Table 2) used in this study.

Each primer was purchased from Thermo Fischer Scientific and each siRNA was purchased from Sigma Aldrich. Primers were the self-designed based on template sequences and siRNAs were designed by siDirect. Three candidates were selected and assayed, the best one for each gene was used in this study and shown here.

Acknowledgements

First of all, I would like to thank Professor Dr. Mikiko C. Siomi as a supervisor. She planned the research and experiments, advised me anytime and coached me how to get the best and clearest data with quite warm heart. Moreover, please let me thank Assistant Professors Dr. Hirotsugu Ishizu, Dr. Kaoru Sato and Dr. Kazumichi M. Nishida. Furthermore, I must thank postdocs Dr. Yukiko Murota and Dr. Ryo Murakami. These five doctors always kindly advised me and showed the direction of my research and experiments. Especially, Dr. Murota was a co-worker and she helped me performing the limited proteolysis assay, which is one of the key experiments in this study. So, if she didn't help me, I couldn't write this and graduate here. I would like to say greatly thank you for her. And I should not forget Dr. Nishida. He helped me performing the binding assay by IP between Imp α and Piwi, which is also the key experiment of this study. He also supported antibody production. If there were no anti-Imp α antibodies, I could not complete this study. His contribution is uncountable.

Of course I don't forget my colleagues. They all are very clever and their intelligence was always helped me. Sometimes they teased me, but sometimes they encouraged me. They are also the pieces that must not lack for completing this study.

Finally, I would like to thank my family for always encouraging me, worrying me and giving me food or living or financial support.

Here I could complete my research and thanks to many people, I could concentrate on the experiments.

Thank you very much.